James B Duncan Jr
https://doi.org/10.5194/wes-2019-78-RC1

General Response

Thank you for your comments and the time taken to provide this review. Please find in this document a response to your specific comments. The authors are confident the responses provided will clear up any confusion or concerns regarding the methods used. Please find as supplemental material an edited version of the manuscript with changes tracked.

Foremost, the authors would like to state that at the time of the experiment (14 December 2014), experimental validation of wind plant control at full scale was rare. Similarly, there was a dearth of observational data (especially compared to numerical simulation) characterizing in three-dimensions wind turbine wake structure and variability. Therefore, in collaboration with an industry partner, the preliminary objectives of the experiment were to (1) examine three-dimensional wind turbine wake response to changes in wind turbine yaw and blade pitch and (2) examine how these changes impact the net power production of individual turbines in the wind plant (i.e. quantifying the effectiveness of the wind plant control strategy). However, experimental logistics (e.g. experimental control limitations imposed by the wind plant operator) ultimately inhibited execution of these experimental objectives. Therefore, experimental objectives and analysis focus evolved to exploring the complexities and difficulties associated with performing a wind plant control experiment at full scale. The results of this study lend insight into these difficulties, and therefore, should be used to inform future field campaigns. The authors are confident the changes made in response to your comments allow the manuscript to tell a more direct story.

Specific Comments

Pg. 2, ln. 17: Double check your references listed. For example, Vollmer et al. 2016 and Fleming et al., 2018 are listed as wind tunnel experiments, but these are numerical simulations.

Vollmer et al. (2016), Fleming et al. (2018), and also Park and Law (2016) were based on numerical simulation. By mistake, these works were initially miscited in the manuscript as studies based on wind tunnel experiments. Furthermore, although Jiménez et al., (2010) leverages the results of previously performed wind tunnel experiments, a significant portion of the manuscript was based on numerical simulation. The citing of these manuscripts was appropriately modified in the manuscript and the authors are confident that the referenced works are now properly cited.

The text now reads (Pg. 2 Lns. 15 through 20):

> "The benefit of wind plant control has been previously demonstrated using numerical simulation (e.g. Jiménez et al., 2010; Johnson and Fritsch, 2012; Lee et al., 2013; Annoni et al., 2015; Park and Law, 2015; Fleming et al., 2015; Gebraad and van Wingerden, 2015; Gebraad et al., 2016; Park and Law, 2016; Vollmer et al., 2016; Fleming et al., 2018; Kanev et al., 2018) and in wind tunnel experiments (e.g. Parkin et al., 2001; Corten and Schaak, 2003; Howland et al., 2016; Schottler et al., 2017; Bartl et al., 2018; Bastankhah and Porté-Agel, 2019)."

Furthermore, the reference for Fleming et al. (2019) has been updated to reflect its status being upgraded from 'In Review' to 'Published'.

Pg. 2, ln. 22: Another recent full-scale validation of wind plant control is: Howland et al, Wind farm power optimization through wake steering, Proceedings of the National Academy of Sciences, 2019.

Thank you for bringing this work to our attention, it is now cited in the manuscript (Pg. 2 Ln 19). Furthermore, based on your input the authors discovered another relevant study by Howland wherein wind tunnel experiments were used to examine the impact of yaw operation on wake structure. This work (documented below) is now referenced in the manuscript.

Howland, M. F., Bossuyt, J., Martínez-Tossas, L. A., Meyers, J., and Meneveau, C.: Wake structure in actuator disk models of wind turbines in yaw under uniform inflow conditions, Renew. Energ. Sustain. Dev., 8, 043301, 2016.

Pg. 2, ln. 25: "To expand upon existing full-scale validation efforts, agreements were made with an industry partner..." Please be sure to review the existing full-scale validation efforts and explain how the present work fits in.

As mentioned in the manuscript, full-scale validation of wind plant control remains limited. Despite the potential benefit of wind plant control being demonstrated in both numerical simulation and wind tunnel experiments, full-scale validation of these control techniques must be performed before wind plant control can be commercially employed.

Based on your comment, the authors recognize that the phrasing,

> "To expand upon existing full-scale validation efforts, agreements were made with an industry partner to modify the yaw and blade pitch of a utility-scale wind turbine for a limited time period to examine the resulting variations in wake structure."

is vague when it comes to defining exiting full-scale validation efforts, and also does not denote how the presented research expects to contribute to the research field.

Existing experimental validation of wind plant control at full-scale has nominally focused on either (1) quantifying the benefit of wind plant control by analyzing the power and controls data of individual turbine pairs in a wind plant over extended periods (e.g. Fleming et al., 2017a; Ahmad et al., 2019; van der Hoek et al., 2019; Fleming et al., 2019; Howland et al., 2019) or (2) using advanced measurement technologies (e.g. lidar) to examine near-wake response to turbine control changes (Trujillo et al., 2016; Fleming et al., 2017b).

The referee should consider the date of the experiment (14 December 2014) when factoring in how this research fits into the now currently published research. The initial focus of the manuscript was not to necessarily build on any specific experimental field campaigns (very few experimental studies were published at this time), but rather to contribute to the general dearth of full-scale experimental datasets examining wind plant control and its efficacy. The preliminary objectives

of this experiment were to (1) examine three-dimensional wind turbine wake response to changes in wind turbine yaw and blade pitch in both the near- and far-wake regions and (2) examine how these changes impact the net power production of individual turbines in the wind plant (i.e. quantifying the effectiveness of the wind plant control strategy). However, experimental objectives evolved based on the experimental difficulties encountered. Analysis focus ultimately evolved to exploring the complexities and difficulties associated with performing a wind plant control experiment at full scale.

However, the authors recognize that the principal objectives of this experiment were not properly reflected in the manuscript by simply stating 'To expand upon existing full-scale validation efforts...'. Therefore, the manuscript text was modified to (1) briefly highlight the state of experimental wind plant control validation at full-scale and (2) to better describe the experimental objectives of the 14 December 2014 experiment. The authors are confident the modified text (copied below) more accurately defines the scope and contents of the manuscript.

Pg. 2 Lns. 24 through 34 and Pg. 3 Lns 1 through 2:

> "Experimental validation of wind plant control at full-scale has frequently relied upon the analysis of power and controls data from individual turbine pairs in a wind plant to quantify the benefit of various wind plant control techniques (e.g. Fleming et al., 2017a; Ahmad et al., 2019; van der Hoek et al., 2019; Fleming et al., 2019; Howland et al., 2019). However, few studies have used advanced measurement technologies (such as lidar or radar) to document differences in wake structure due to the turbine control changes implemented as part of wind plant control (e.g. Trujillo et al., 2016; Fleming et al., 2017b). Additionally, these studies almost exclusively limit wake measurement to the near-wake region, and therefore, are unable to monitor the downstream progression of these control-induced wake modifications. To contribute to these full-scale validation efforts, and to expand the downstream extent to which control-induced wake changes are measured, agreements were made with an industry partner to modify the yaw and blade pitch of a utility-scale wind turbine for a limited time period to examine the resulting variations in wake structure. Wake measurements were made using Texas Tech University's Ka-band (TTUKa) Doppler radars employing dual-Doppler (DD) scanning strategies. However, rather than validating the effectiveness of these wind plant wake-mitigating control strategies, results highlight some of the complexities associated with executing and analysing wind plant control strategies at full-scale using brief experimental periods."

Section 2.2: Can you explain if the 12 October experiment is at a different site? Are both sites in similar terrain, or are there significant differences between them that should be pointed out.

The 14 December 2014 and 12 October 2015 radar experiments were performed at different sites. This is in part why instrumented tower data was available for the 12 October 2015 SD radar deployment but not for the 14 December 2014 DD radar deployment. However, both sites were located in the US Great Plains and there were no significant terrain differences between the two sites that would impact wind plant complex flow structure or variability. Although confidentiality agreements preclude disclosure of the radar deployment locations, manuscript text was modified

to provide more details regarding the general location (i.e. the US Great Plains) of the two radar deployments.

Pg. 3 Lns. 23 through 24 now reads:

> "The technical specifications of the TTUKa radars are further detailed in Table 1 and radar deployment specifics (both performed in the US Great Plains) are provided in the subsections below."

Fig. 1: Please explain the meaning of the different colors of wind turbines, including white, to avoid confusion.

A brief description of the turbines was provided in the in the initial manuscript submission in the first paragraph of Section 3.

Pg. 5 Lns. 11 through 16 and Pg. 6 Lns. 1 through 2:

> "Located in the DD domain of the 14 December 2014 deployment were 20 wind turbines distributed across two turbine rows. The wind turbines were characterized by a hub height of 80 m and a rotor diameter (RD) of 101 m. Supervisory control and data acquisition (SCADA) information detailing the turbine inflow wind speed (subject to the nacelle transfer function [NTF]), turbine yaw orientation, and blade pitch angle were provided at a one-hertz sampling frequency from 14:00:00 UTC to 16:59:45 UTC for seven of the wind turbines (denoted by the non-black circles in Fig. 1). Three of the seven wind turbines were located in the leading row of the wind plant, while the remaining four were located in the trailing row. The three lead-row wind turbines were separated by an average distance of 1512.2 m (~15 RD) from the trailing turbine row and were laterally separated from each other by an average distance of 321.1 m (~3 RD)."

However, the authors recognize that this text is disconnected from the description of the 14 December 2014 radar deployment (i.e. Section 2.1) and Fig. 1. Therefore, this text was moved to the end of Section 2 and was also slightly modified to better explain the figure (in particular the meaning of the different color turbines). Furthermore, both the caption and legend to Fig. 1 were modified to improve reader comprehension. The revised text is copied below for reference.

Pg. 4 Lns. 14 through 23:

> "Located in the DD domain of the 14 December 2014 deployment were 20 wind turbines distributed across two turbine rows. The wind turbines were characterized by a hub height of 80 m and a rotor diameter (RD) of 101 m. Supervisory control and data acquisition (SCADA) information detailing the turbine inflow wind speed (subject to the nacelle transfer function [NTF]), turbine yaw orientation, and blade pitch angle were provided at a one-hertz sampling frequency from 14:00:00 UTC to 16:59:45 UTC for seven of the wind turbines (denoted by the non-black circles in Fig. 1). Three of the seven wind turbines were located in the lead row of the wind plant (denoted by the blue, red, and purple circles in Fig. 1), while the remaining four were located in the trailing row (denoted by the white circles in Fig. 1). The three lead-row wind turbines were separated by an average distance of 1512.2 m (~15 RD) from the trailing turbine row and were laterally separated from each other by an average distance of 321.1 m (~3 RD). The wake of these

three lead-row wind turbines (referred to as the T_L, T_T, and T_R) were analyzed to examine the effectiveness of the implemented wake-mitigating control strategies."

Pg. 6, ln. 1: What purpose do the downstream turbines (white circles) serve in this experiment.

SCADA data from the four downstream turbines were used along with SCADA data from the three lead-row wind turbines to estimate the region three pitch schedule used in analyses. This was indicated in Sect. 3.1.1 of the initial manuscript submission.

Pg. 7 Lns 13 through 16:

"Data from all seven wind turbines were used to ensure a robust estimate of the region three pitch schedule (a total of 41,343 SCADA wind speed and blade pitch angle measurements were used); measurements inconsistent with region three pitch operation and T_T data from the experimental periods were not considered when constructing the pitch schedule."

However, to improve reader comprehension, the manuscript text was slightly modified to that copied below.

Pg. 7 Lns 29 through 32:

"Data from all seven wind turbines with SCADA information provided (i.e. the non-black circles in Fig. 1) were used to ensure a robust estimate of the region three pitch schedule (a total of 41,343 SCADA wind speed and blade pitch angle measurements were used); measurements inconsistent with region three pitch operation and T_T data from the experimental periods were not considered when constructing the pitch schedule."

Pg. 6, ln. 18: Fleming et al., 2018 deals with numerical simulations, do you mean 2019?

Thank you for noticing this, the text was appropriately modified to Fleming et al. (2019).

Pg. 7, ln. 6: If the benefit of modifying blade pitch is greater in region 2, then why was the sole half-hour experiment period in region 3? Would have it made more sense to wait for more favorable conditions?

The wind plant control experiment would have been ideally performed for extended experimental durations and in an environment more conducive to the effectiveness of the implemented control strategies. However, experimental logistics ultimately inhibited execution of the experiment when conditions were optimal. These logistical difficulties are detailed below.

Foremost, although the TTUKa radars can comprehensively document wind plant complex flow structure and variability at high spatial resolutions, data availability is dependent on the atmospheric conditions present (namely the size distribution of scatterers and aerosols present in the ABL). This dependency is also true for other remote sensing instrument such as lidar. Given the specifications of the TTUKa radars, data availability is enhanced in certain precipitating

environments. Therefore, wind plant control experiments were limited to periods when the TTUKa radars were expected to have sufficient data availability. Further impacting rapid radar deployment when atmospheric conditions were ideal was the relative proximity of the wind plant to the staging (i.e. storage) location of the radars. The wind plant was located several hundred miles away from the TTUKa radars when not in use. Therefore, accurate forecasts of atmospheric conditions conducive to data availability had to be made with sufficient lead time to (1) enable proper coordination with the wind plant operators (control experiments were not permitted at all times) and (2) to deploy the radars to the wind plant site. Successful execution of the wind plant control experiment was therefore not as simple as waiting for conditions to become ideal. Furthermore, periods conducive to data availability were not necessarily correlated with atmospheric conditions conducive to the effective implementation of wind plant control (as demonstrated in the manuscript).

However, the 14 December 2014 deployment was not the only attempt at performing a wind plant wake mitigation control experiment. Wind plant control experiments were also performed at a wind plant elsewhere in the US Great Plains and at the TTU Scaled Wind Farm Technology (SWiFT) facility (albeit this is a scaled wind farm facility). The 14 December 2014 radar deployment was presented in this manuscript in part because the wind plant operator allowed a relatively wide range of experimental turbine control changes to be implemented. Prior to recent years, some wind farm operators were reluctant to collaborate on these types of experiments for fear that implementing wind plant wake-mitigating control techniques might impact turbine warranty.

Finally, this field experiment, albeit performed in somewhat of a suboptimal environment and having inherent limitations, lends insight into the complexities associated with performing a full-scale wind plant control experiment. The authors are confident this manuscript adds value to the scientific community and can be used to inform future field campaigns.

Pg. 7, ln. 9: "To maintain the rated generator speed in region three, the wind turbine follows a pitch schedule to extract the desired amount of momentum at various wind speeds." Blade pitch controllers typically use generator speed feedback to control blade pitch to regulate generator speed. Therefore, if you are adding a pitch offset in region three, what else are you changing in the controller so that the pitch controller doesn't simply compensate for the offset to bring the generator speed back to rated? Is the generator torque or generator speed setpoint also changed? Could it be that the pitch offset that is added is simply an offset to the "fine pitch" (minimum pitch) angle that the turbine operates at below rated, and that there is no real change to the pitch control above rated? More detail about the intended pitch offset strategy would be helpful.

Due to the proprietary nature of the information, the construct of the wind turbine controller was not provided by the turbine manufacturer. Therefore, the authors are unable to expand on the blade pitch angle offset strategy, nor are they able to state with confidence why these changes were not effectively implemented. This is reflected in the manuscript on Pg. 7 Lns. 3 through 5:

> "Not having access to wind turbine controller design is a major challenge to fully understanding wind turbine behaviour (Fleming et al., 2019), or rather, how the controller

> responds to variable inflow conditions when attempting to enact the desired control offsets. Therefore, the provided discussions do not detail why the turbine was able or unable to enact the desired control changes, but rather focuses on quantifying the resulting offsets."

However, it was the author's understanding that the blade pitch angle offsets (i.e. +1°, +2°, +3°) were implemented independent of the inflow state and operation of the turbine (i.e. region two or three).

The referee indicates that generator speed (i.e. rpm) is typically used to help regulate wind turbine blade pitch. Therefore, even if blade pitch were directly modified by incorporating the blade pitch angle offset, the turbine might recognize inconsistent generator speeds relative to the turbine inflow wind speed and appropriately modify the blade pitch. However, regardless of whether generator speed was relied upon to help regulate blade pitch, experimental mean blade pitch angle offsets were not negligible (i.e. Figs. 3 and 4 of the manuscript). Experimental period (i.e. +1°, +2°, +3°) generator speed behavior was also examined to try and gain a more comprehensive understanding of the implemented control changes. However, analyses did not lend much insight, and therefore, these analyses were not incorporated into the manuscript.

Pg. 7, ln. 12: "The region three pitch schedule was constructed by fitting a linear model to the distribution of blade pitch angles..." Pitch schedules are generally very nonlinear as a function of wind speed, especially near rated wind speed. Can you elaborate on your choice of a linear pitch schedule model?

Pg. 7 Lns. 29 through 32:

> "Data from all seven wind turbines with SCADA information provided (i.e. the non-black circles in Fig. 1) were used to ensure a robust estimate of the region three pitch schedule (a total of 41,343 SCADA wind speed and blade pitch angle measurements were used); measurements inconsistent with region three pitch operation and T_T data from the experimental periods were not considered when constructing the pitch schedule."

The constructed region three blade pitch schedule is provided below (note: due to confidentiality agreements the blade pitch angle values could not be plotted along the y-axis). In this figure, there is a rough linear relationship between blade pitch and the region three turbine inflow wind speeds. However, detracting from this linear relationship is a small magnitude of clustering in blade pitch between 12 and 13 m s^{-1}. This clustering is believed to occur as a result of a rapid increase (i.e. at timescales less than the response time of the blade pitch controller) in the turbine inflow wind speed from velocities consistent with region two to region three. Within this period, the turbine is unable to appropriately modify its blade pitch angle to be consistent with region three pitch operation. While it would be desirable to remove these measurements, these values are surrounded by blade pitch angle measurements consistent with region three pitch operation and only represent 1.19 % of the total number of measurements considered. Therefore, this clustering is not expected to significantly impact the construction of the region three pitch schedule.

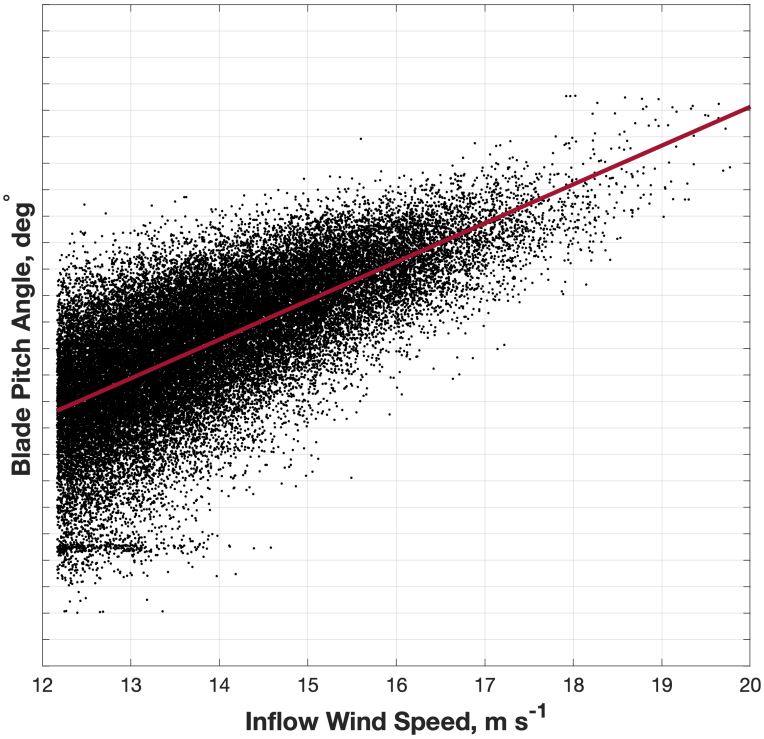

The authors are confident that these methods enable a robust best-estimate of the region three pitch schedule. Further confidence can be placed on these methods based on the results of Duncan et al. (2019).

Duncan, J. B., Hirth, B. D., and Schroeder, J. L.: Enhanced estimation of boundary layer advective properties to improve space-to-time conversion processes for wind energy applications, Wind Energ., 22, 1203-1218, 2019.

In Duncan et al. (2019), this pitch schedule was used to estimate variations in generator speed due to suboptimal blade pitch angle activity.

Pg. 9, ln. 12: A 1.45 km by 1.8 km averaging area seems too large for determining the local inflow wind direction to the turbines, especially if you are trying to distinguish between the wind inflow to each of the three turbines. Furthermore, given the advection time across the 1.8 km analysis area, the estimated wind directions are likely not very well correlated with what the turbines see at a high temporal resolution. Can you try this with 100 m x 100m averaging areas, local to each turbine? This could improve your results, or at least make things more meaningful.

The referee contends a 1.45 km by 1.8 km averaging area is too large to discern turbine-specific inflow differences. Therefore, the referee argues the value of θ_{inf}^{V} will likely not be well correlated with the turbine inflow wind direction at higher temporal resolutions. In order to more accurately resolve turbine inflow conditions, the referee recommends using a 100 m by 100 m averaging area local to each turbine. However, due to the interpretation of the DD synthesized wind fields, this 100 m by 100 m turbine-local averaging area is also not necessarily appropriate. Denoted on Pg. 3

Ln. 30 and Pg. 12 Ln 9, the TTUKa radars take on average 60.4 s to collect a single DD volume, and within this DD volume acquisition period, turbulent structures move. Therefore, denoted in Sect. 2.1, Pg. 4 Lns. 5 through 7:

> "The DD wind maps can be interpreted as a pseudo-average of the wind conditions over the volume acquisition period, where the DD volume time stamp denotes the end of the volume period."

Space-to-time conversion techniques (e.g. Duncan et al., 2019) are required to accurately resolve temporal inflow variability at sub-volume timescales (i.e. less than the measurement revisit period). Using local measurements without a proper understanding of how turbulent structures move within the DD volume acquisition period can confound results. Ideally, space-to-time conversions would have been used in Sect. 3.2 to develop a semi-continuous stream of turbine inflow information (wind speed and direction) over the DD volume acquisition period. This would have allowed for temporal inflow variability to more accurately defined, and therefore, would have enabled a more comprehensive determination of the implemented control changes. Denoted on Pg. 12 Lns. 11 through 16:

> "To improve controller assessment, future field campaigns should place precedence on turbine inflow measurements (wind speed and direction) independent of the turbine control system (i.e. non-SCADA data). Experiments using scanning-based measurements should use advanced analysis techniques, such as those established in Duncan et al. (2019) wherein space-to-time conversions were performed on the spatially distributed velocity fields, to provide a comprehensive characterization of the turbine inflow wind speed and direction on a second-by-second basis. Application of these methods was limited because of data availability issues."

These methods were not employed because of data availability issues. While a more local turbine inflow estimate (specifically laterally) might have slightly improved result accuracy, the use of a larger-scale averaging area does not reduce the meaningfulness of the results. Given the average time between DD volume scans (i.e. 60.4 s) and the mean wind speed within the DD analysis period (i.e. 13.71 m s^{-1} as defined by the mean wind field within the freestream analysis area), a relatively large averaging area is not a bad estimate of the mean conditions observed at the turbine over the DD volume acquisition period. While the freestream analysis area is still larger than the longitudinal wind field area that might advect through the turbine over the DD volume acquisition period (based on Taylor's hypothesis this would be a distance of 828.1 m [i.e. 60.4 s x 13.71 m s^{-1}]), differences between these two inflow estimates are not expected to be significant.

Regardless, analysis was performed to demonstrate the sensitivity of the turbine inflow estimate to the averaging area used. Comparisons were made between the turbine inflow wind direction determined using (1) the freestream analysis (i.e. $\theta_{\mathrm{inf}}^{V}$) and (2) local turbine averaging areas representing the estimated portion of the upstream wind field that will advect through the turbine over the subsequent volume acquisition period based on Taylor's hypothesis. A comparison of these different inflow estimates at 15:31:00 UTC is demonstrated in the figure below. The left subplot demonstrates the spatial dimensions of the individual averaging areas at 15:31:00 UTC, while the right subplot demonstrates the turbine inflow wind direction profile derived from these

averaging areas. The profile-averaged turbine inflow wind direction is provided in the legend of the right subplot for each averaging area. Despite analyzing significantly different areas (especially laterally), differences between the turbine inflow wind direction estimates were small. At 15:31:00 UTC, the T_L inflow wind direction was 0.7° greater than the value of θ_{inf}^{V}, the T_T inflow wind direction was equal to the value of θ_{inf}^{V}, and the T_R turbine inflow wind direction was 1.2° less than the value of θ_{inf}^{V}.

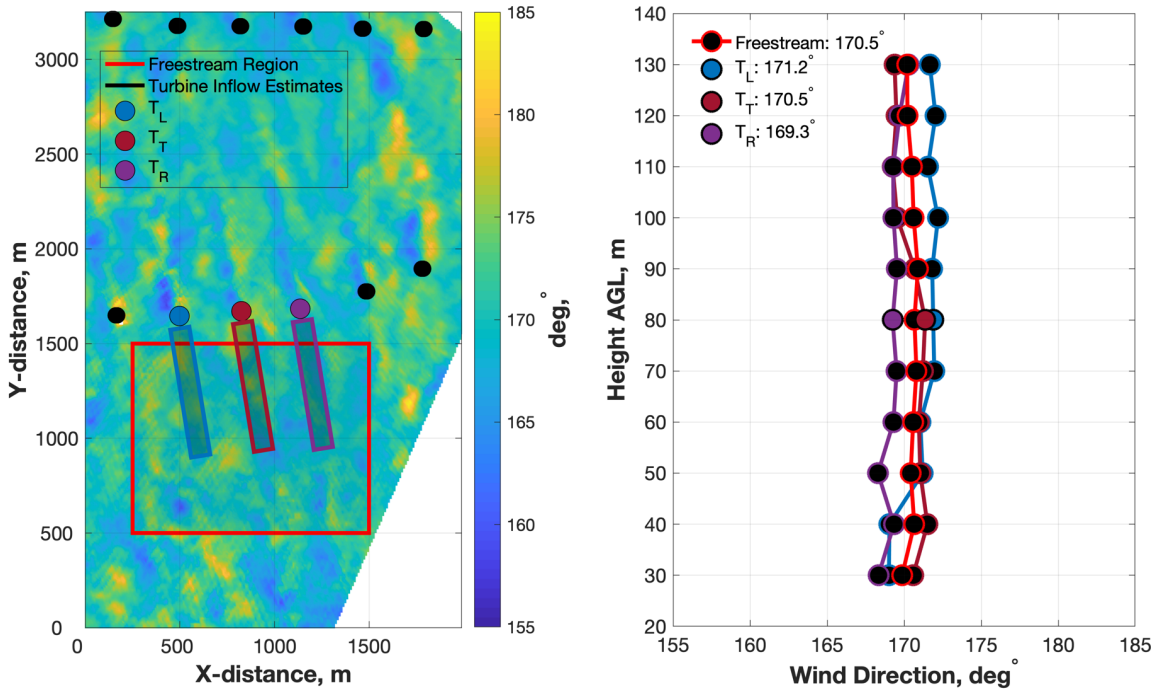

The same analysis was performed for each DD volume in the analysis period to demonstrate that these small differences were not rare. Time histories of θ_{inf}^{V} and the local turbine inflow estimates are provided in the figures below for each turbine. The black lines denote the θ_{inf}^{V} time history and the colored lines denote the local turbine inflow estimates. The local turbine averaging areas were redefined in each DD volume using Taylor's hypothesis based on the mean conditions in the freestream analysis area. While Taylor's hypothesis was used to give a general idea of the sensitivity of the turbine inflow estimate to the averaging area used, the referee should refer to Duncan et al. (2019) for why Taylor's hypothesis cannot be systematically relied upon to accurately denote the advection of the upstream wind field and hence why these techniques were not used in the manuscript.

Provided in the legend of each figure are both the mean deviation and the mean absolute deviation between θ_{inf}^{V} and the local turbine inflow estimates for the entire DD analysis period. Time history data gaps are due to data availability issues; at least 50 % of the respective averaging area was required to determine the mean wind direction estimate. Considering inflow estimate data from all turbines and DD volumes, the mean deviation between the two turbine inflow estimates (the local turbine inflow estimate minus the value θ_{inf}^{V}) was -0.2° and the mean absolute deviation was 1.1°. These results do not indicate that the use of the freestream analysis area to estimate the turbine

inflow wind direction (i.e. θ_{inf}^{V}) reduced the meaningfulness of the results. However, the authors do acknowledge that analyses would have benefited from more accurate turbine inflow estimates.

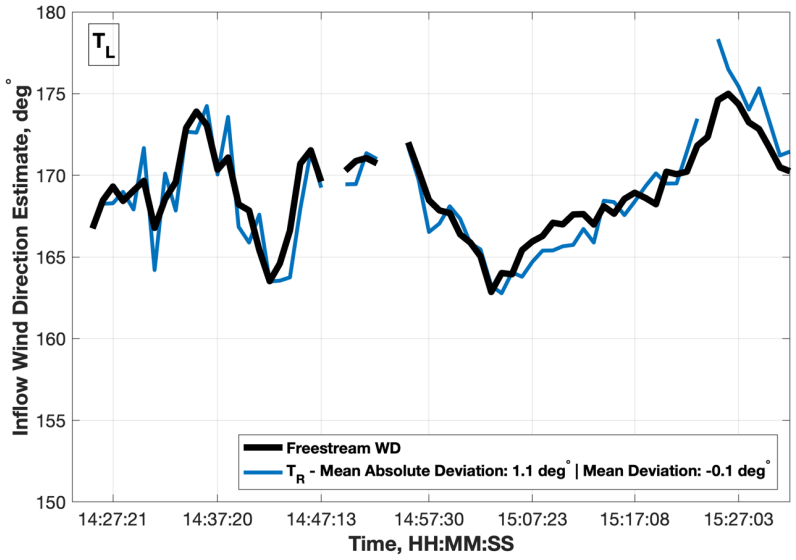

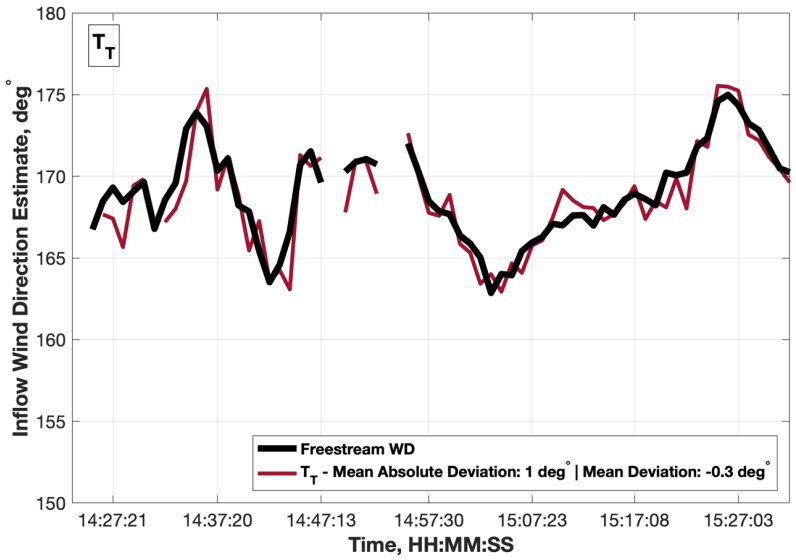

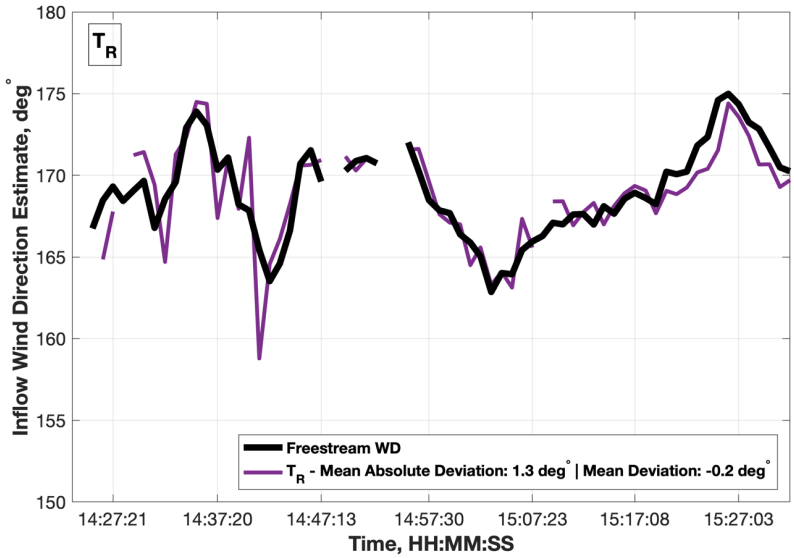

Furthermore, the use of the freestream analysis area to estimate the turbine inflow wind direction provides a common reference frame for defining both the wake (i.e. θ^{V}_{skew}) and streak (i.e. $\theta^{V}_{\text{S-skew}}$) skew angles.

Section 3.1.2: Given the large positive mean yaw errors with or without the offset applied, it seems possible that the yaw position reported in the SCADA data is not calibrated properly. It is common for yaw position values from SCADA data to deviate significantly from the true orientation (i.e., 0 degrees -> true north) over time. If not, this should be discussed further.

The referee raises the concern that yaw calibration errors might have impacted results because improper yaw calibration is not uncommon. Although not discussed in the manuscript, analysis was performed to discern whether a yaw calibration error was present in either the T_L, T_T, or T_R.

Foremost, regardless of any yaw calibration error, variations in yaw error (i.e. θ^{V}_{err}) should elicit distinct changes in wake skew (i.e. θ^{V}_{skew}). Counterclockwise rotor rotation relative to a fixed turbine inflow wind direction (i.e. a net positive increase in θ^{V}_{err}) should enhance wake deflection to the right when looking downstream (i.e. resulting in a net increase in θ^{V}_{skew}), and clockwise rotor rotation relative to a fixed turbine inflow wind direction (i.e. a net negative decrease in θ^{V}_{err}) should enhance wake deflection to the left when looking downstream (i.e. resulting in a net decrease in θ^{V}_{skew}). However, demonstrated in Fig. 10b and the figure below, it is tough to discern any distinct trends in θ^{V}_{skew} resulting from variations in θ^{V}_{err}. Based on the figure below, it appears as though the value of θ^{V}_{skew} slightly decreased as the value of θ^{V}_{err} increased. However, when data from all three turbines is considered (i.e. Fig. 10b), and thereby a wider range of θ^{V}_{err} values considered, this relationship was not as apparent. Therefore, yaw calibration errors cannot explain the general insensitivity of in θ^{V}_{skew} to variations in θ^{V}_{err}.

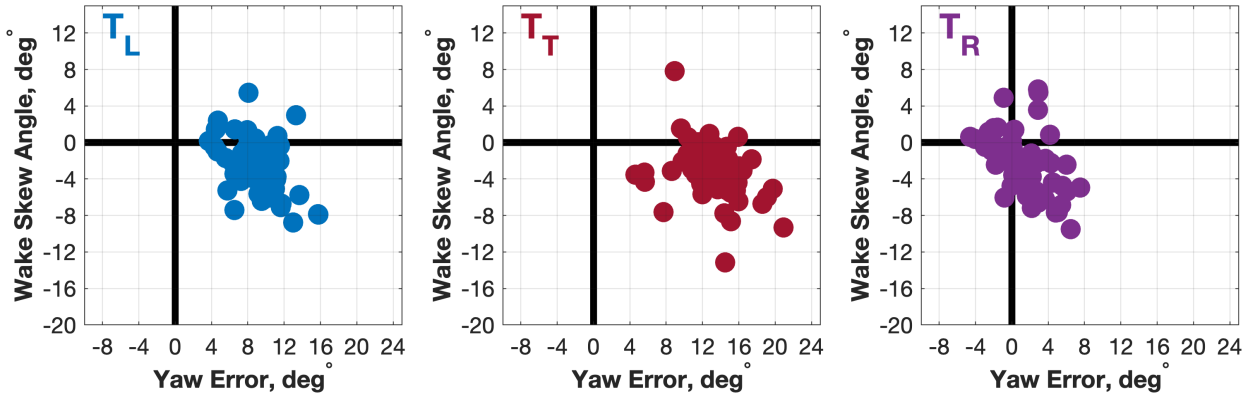

Alternatively, assume each turbine has a yaw calibration error and therefore is generally well aligned with the inflow wind direction in the DD analysis period (i.e. each turbine exhibits a mean θ^V_{err} value of 0°). If this is true, then the wake of each turbine should roughly extend linearly downstream an angle consistent with the value of θ^V_{inf}. To examine whether the wind turbine wakes were extending linearly downstream, the T_L, T_T, and T_R wake orientation angles (i.e. θ^V_{wake}) were compared to value of θ^V_{inf} in the figure below.

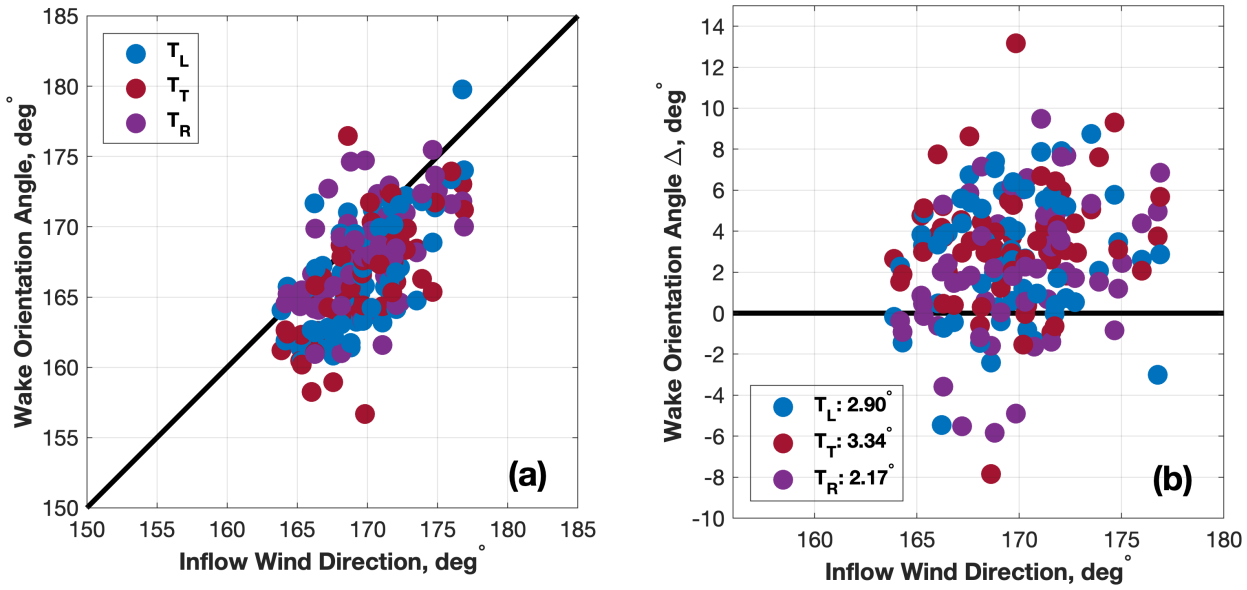

The left subplot demonstrates the values of θ^V_{wake} were consistently less than the volume-respective value of θ^V_{inf}. Therefore, the wake centerlines were on average skewed to the left of their expected location based on the value of θ^V_{inf} and an assumed θ^V_{err} value of 0°. The right subplot demonstrates the difference between the T_L, T_T, and T_R θ^V_{wake} values and the value of θ^V_{inf}. On average, the T_L θ^V_{wake} value was offset of θ^V_{inf} by -2.90°, the T_T θ^V_{wake} value was offset of θ^V_{inf} by -3.34°, and the T_R θ^V_{wake} value was offset of θ^V_{inf} by -2.17°. Negative values indicate wake skew to the left when looking downstream. Because the values of θ^V_{wake} were inconsistent with the volume-respective value of θ^V_{inf}, and also because the θ^V_{skew} values demonstrated little sensitivity to variations in θ^V_{err}, yaw calibration errors were not expected to have a significant impact on the presented results.

To provide the reader with more confidence that yaw calibration errors did not adversely impact the results, text was added to the manuscript.

Pg. 17 Lns. 2 through 4

> "Furthermore, the values of θ_{skew}^{V} were inconsistent with θ_{inf}^{V}, which along with the weak correlation between θ_{skew}^{V} and θ_{err}^{V} provides confidence that the unexpected mean sign of θ_{skew}^{V} was not simply a result of a turbine yaw calibration error."

Pg. 11, ln. 15: 'However, nacelle-based measurements are inherently distorted...' Another factor to consider is that the flow distortion from the rotor can change as the control changes. Adding a pitch offset could cause the wind speed behind the rotor to change differently than with the original control, complicating the detection of changes in turbine operation as a function of wind speed.

The referee indicates that experimental turbine control changes could impact the validity of the nacelle-transfer function (NTF). These turbine control changes could modify typical flow distortion levels behind the rotor, thereby reducing the effectiveness of the NTF used to convert the nacelle-mounted anemometer measurement to a rotor-effective inflow velocity. Therefore, experimental control changes could also impact detection of the control changes implemented when analyzed as a function of the NTF-based inflow velocity. As denoted prior, this demonstrates the need for more accurate turbine inflow estimates, in particular measurements that are independent of the turbine control system. Manuscript text was slightly modified to reflect the need for these types of measurements.

Pg. 12 Lns. 11 through 16:

> "To improve controller assessment, future field campaigns should place precedence on turbine inflow measurements (wind speed and direction) independent of the turbine control system (i.e. non-SCADA data). Experiments using scanning-based measurements should use advanced analysis techniques, such as those established in Duncan et al. (2019) wherein space-to-time conversions were performed on the spatially distributed velocity fields, to provide a comprehensive characterization of the turbine inflow wind speed and direction on a second-by-second basis. Application of these methods was limited because of data availability issues."

Pg. 12: ln. 10: 'Both of these factors might have contributed to the experimental control offsets not being fully realized.' Certainly for yaw control, a single 10-minute period might not be sufficient to observe meaningful yaw misalignment changes, given the slow dynamics of yaw controllers.

Additional text was added to the manuscript to better convey this message.

Pg. 12 Lns. 25 through 27:

> For example, the brief duration of the experimental periods may have been insufficient to realize/validate the desired control offsets (in particular the ability to observe significant yaw misalignment changes), and the ability to implement the desired control

changes might have been impacted by the ABL conditions present (e.g. region three inflow wind speeds).

Section 4.1: I would suggest a revised wake tracking algorithm in light of improvements in the understanding of wake deflection physics. As discussed in papers such as the following, yaw misalignment can cause wakes to have a 'curled' shape due to the presence of counter rotating vortices. This means the peak velocity deficit could change with height and averaging across all heights in the rotor disk area is not necessarily the most relevant metric.

- **Vollmer et al. Estimating wake deflection downstream of a wind turbine in different atmospheric stabilities: an LES study, Wind Energy Science, 2016**

- **Howland et al, Wake structure in actuator disk models of wind turbines in yaw under uniform inflow conditions, Journal of Renewable and Sustainable Energy, 2016.**

- **Fleming et al., A simulation study demonstrating the importance of large-scale trailing vortices in wake steering, Wind Energy Science, 2018.**

A more meaningful lateral wake center estimate for wind plant control applications can be found using the method explained in Vollmer et al. 2016, where the cubed wind speed is averaged across a hypothetical rotor disk area centered at different lateral displacements. The displacement that results in the lowest value can be considered the wake center position.

The referee contends the employed wake-tracking algorithm might not have adequately resolved lateral wake center location because of the impact yaw misalignment can have on wake structure. However, before addressing this concern, the authors would like to clarify the methods used in the wake-tracking algorithm. The referee states 'averaging across all heights in the rotor disk area is not necessarily the most relevant metric'; however, no averaging was used in the wake-tracking algorithm. Instead, at each constant-height plane within the wind turbine rotor sweep, the horizontal location of the wind speed minimum was determined and the median (not mean) horizontal location of these minima was used to discern the lateral wake center location.

Regardless, an analysis was performed to examine whether the operational yaw errors modified wake shape. Both numerical simulation and wind tunnel testing demonstrate rotor-sweep relative variations in wind turbine thrust caused by yaw error can promote a kidney-shaped (or curled) wake (e.g. Churchfield et al., 2016; Vollmer et al., 2016; Bartl et al., 2016). Therefore, wake structure changes induced via yaw error could potentially impact the wake-tracking algorithm. To briefly examine changes in wake shape due to yaw error, composite mean wake deficit cross-sections were developed for the T_L, T_T, and T_R using data from all contributing DD volumes in the +10° experimental period.

To determine the composite mean wake deficit cross-section, the vertical wake cross-sections used to identify the wake were first redefined at each distance downstream about the wake center location. Wind speed measurements within the redefined cross-sections were then converted to wake deficit values, defined as the percentage reduction in wind speed from the DD volume freestream wind speed profile. The DD volume freestream wind speed profile was developed by

determining the mean wind speed within the freestream analysis area at each constant-height plane within the wind turbine rotor sweep (i.e. the same as Fig. 5 but for wind speed instead of wind direction). Therefore, the individual wake deficit values (i.e. $v_{deficit}$) were defined by,

$$v_{deficit} = \frac{v_{wake}^{V,h} - v_{inf}^{V,h}}{v_{inf}^{V,h}} \cdot 100$$

where $v_{wake}^{V,h}$ denotes a wake cross-section wind speed measurement at height (h) and $v_{inf}^{V,h}$ denotes the height-respective DD volume freestream wind speed. The wake deficit cross-sections were then averaged at each distance downstream to determine the T_L, T_T, and T_R composite mean wake deficit cross-sections for the +10° experimental period. Wake deficit contours at 10 %, 15 %, and 20 % were used to qualitatively examine wake shape. However, based on this contour analysis at 1 RD downstream (refer to the figure below), neither the wake of the T_L, T_T, nor T_R exhibited a modified (i.e. kidney or curled) shape. The contours are roughly concentric, and thereby denote a near circular wake. The most notable difference between the composite mean wake of the T_L, T_T, and T_R was the relative size of the contours (i.e. indicating differences in wake intensity).

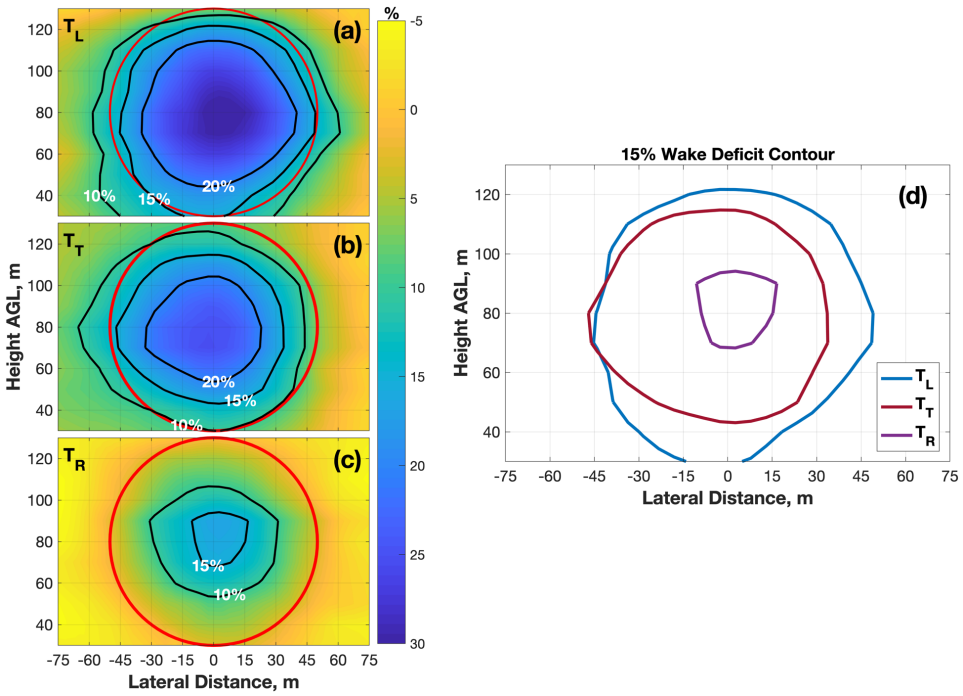

Reference Figure: Composite mean wake deficit cross-sections (presented as a percentage reduction from the DD volume freestream wind speed profile) at 1 RD downstream for the (a) T_L, the (b) T_T, and (c) the T_R. Contours corresponding to a 10 %, 15 %, and 20 % wake deficit are overlaid in black and the wind turbine rotor sweep is overlaid in red. (d) The T_L, the T_T, and the T_R 15 % wake deficit contour at 1 RD downstream.

While this analysis was limited to the +10° experimental period, additional analysis was performed using data from all DD volumes within the DD analysis period (i.e. 14:22:32 UTC – 15:31:57 UTC). At 1 RD, 2 RD, and 5 RD downstream, the mean horizontal (i.e. lateral) location of the wind speed minima (defined relative to the lateral location of the wake center [i.e. +/-]) was determined at each constant-height plant within the wind turbine rotor sweep for the T_L, T_T, and T_R. The mean lateral location of these wind speed minima is denoted in the figures below. Variability about the zero line denotes the average displacement of the height-respective wind speed minima from the wake center. Therefore, changes in wake structure due to yaw error should

be reflected in these mean profiles. Although there were some lateral displacements in the wind speed minima mean location at 1 RD downstream, no mean displacement exceeded 10 m. The observed displacements were not significant enough to indicate extensive wake shape deformation resulting yaw error. These results do not indicate yaw error does not modify wake shape, but suggest the operational yaw error values along with the turbine inflow wind speeds were not significant enough to elicit these changes. Therefore, the effectiveness of the wake-tracking algorithm is not expected to have been adversely impacted by any perceived changes in wake shape resulting from yaw error.

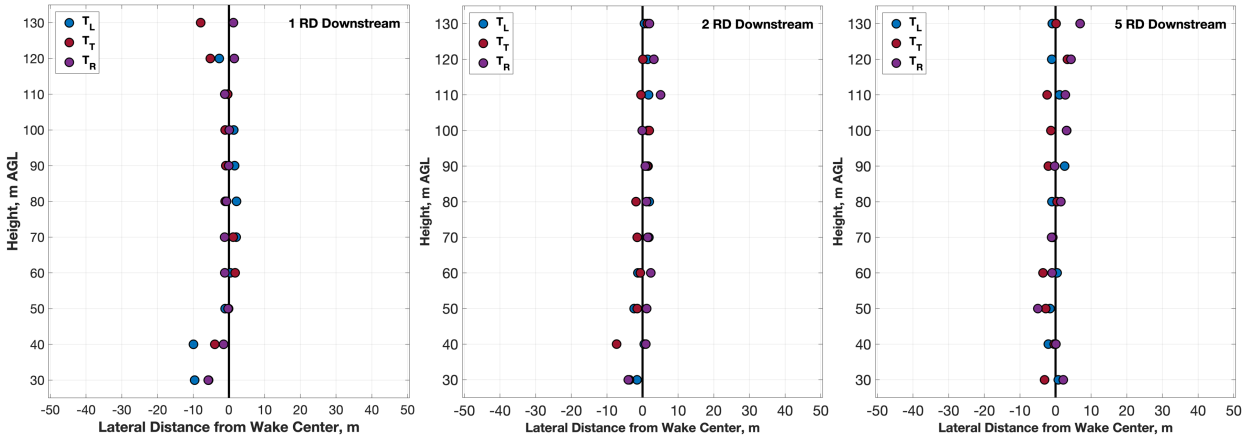

To ease referee concerns regarding the employed wake-tracking algorithm, the referee-recommended wake-tracking algorithm was also applied and analyses was re-ran. The lateral wake center location was determined at each distance downstream by identifying the lateral location that minimized the rotor-sweep disk averaged cubic wind speed. Lateral displacements ranging from -100 m to +100 m at 10-m intervals were examined at each distance downstream. Using this method (refer to the figure below), the T_T wake at 14:33:20 UTC was located -10 m (i.e. to the left when looking downstream) of its expected location based on the inflow wind direction (i.e. θ_{inf}^{V}).

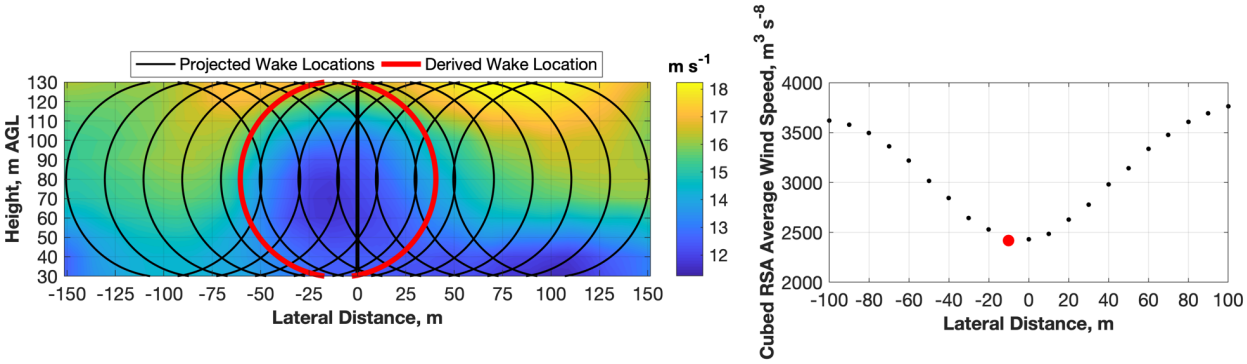

Despite implementing the referee-recommended wake-tracking algorithm, the wake skew values were not significantly modified. With this wake-tracking algorithm applied, all three turbines still exhibited a negative mean wake deflection angle, indicating wake deflection to the left when looking downstream. This is opposite of expected based on the operational yaw error values and theory. Therefore, the choice of wake-tracking algorithm did not impact the take-home message of the wake skew analysis. In order to maintain consistency between the SD and DD wake-tracking

algorithms, the wake-tracking algorithm previously established by Hirth and Schroeder (2013) will be employed.

Fig. 9: Is Fig. 9 (a) showing the distance from the centerline of the wake after corrected for the skew angle, or from the centerline in the mean wind direction. Please clarify what is being shown.

The figure indicates the lateral distance from the wake centerline as defined by θ_{wake}^{V} (i.e. "after corrected for the skew angle"). This is denoted in the first manuscript submission on Pg. 15 Lns. 4 through 5:

> "Constrained linear least-squares regression (Gill et al., 1981) was used to determine the value of θ_{wake}^{V}, wherein the wake centerline was required to emanate from the location of the wind turbine."

To improve clarity, both manuscript and figure text were modified.

Pg. 15 Ln. 13 and Pg. 16 Lns. 1 through 2:

> "The value of θ_{wake}^{V} minimized the error sum of squares; the error distribution was defined as the lateral distance between individual wake center locations and the wake centerline (i.e. θ_{wake}^{V}) (e.g. Fig. 9a)."

Figure 9 Caption:

> **Figure 9.** (a) The lateral distance between the T_T wake centerline (as defined by θ_{wake}^{V}) and the wake center locations (i.e. the T_T error distribution). (b) TTUKa DD hub-height wind speed (m s^{-1}) at 15:30:00 UTC overlaid by the T_L, T_T, and T_R wake centerline and the wake center locations at 1-RD increments.

Pg. 16, ln 6: '...indicating the observed wake deflection...was opposite of that expected.' How might wind veer impact the wake deflection during the experiment period? Could this be an explanation for the unexpected skew?

Wind veer can induce rotor-sweep relative variations in yaw error. In the presence of wind veer, a rotor that is well aligned with the wind at hub height will exhibit increasing magnitudes of yaw error (albeit opposite signs) in the upper and lower halves of the wind turbine rotor sweep. Therefore, a turbine exhibiting minimal yaw error at hub height should produce a wake (as viewed from above) that widens with distance downstream. This perceived wake widening is due to the wake being deflected in one direction (left/right) in the lower half of the rotor sweep and in the other direction (right/left) in the upper half of the rotor sweep. Depending on the veer profile (i.e. veering/backing and intensity [° per m AGL]), wake deflection can either be promoted or inhibited relative to that expected based on the hub-height turbine inflow wind direction and the yaw orientation angle. For this reason, hub-height wind directions cannot comprehensively

quantify the rotor-relative variations in yaw error that contribute to wake deflection. To increase the robustness of the results, a rotor-sweep average wind direction (i.e. θ_{inf}^{V}) was used to quantify yaw error. This was noted in the first manuscript submission on Pg. 9 Lns 16 through 18 and Pg. 10 Lns 1 through 5.

> "Due to wind plant and turbine measurement limitations, yaw error is traditionally defined relative to the hub-height wind direction measured by the nacelle wind vane. However, the nacelle wind vane is unable to account for differences in wind direction with height (i.e. wind veer). Therefore, yaw error defined by the hub-height wind direction will be unable to comprehensively quantify the rotor-sweep relative variations in the axial induction factor that cause wake deflection. Hence, yaw error $\left(\text{i.e. } \theta_{err}^{V}\right)$ was defined in each DD volume relative to the RSA average turbine inflow wind direction using
>
> $$\theta_{err}^{V} = \theta_{inf}^{V} - \theta_{yaw}^{V}$$
>
> where θ_{yaw}^{V} was the DD volume yaw angle (i.e. the mean yaw angle during the DD volume acquisition period). Positive magnitudes of θ_{err}^{V} denote counterclockwise rotor rotation relative to θ_{inf}^{V}."

Prior to examining wind veer in the DD analysis period, it can be noted that the T_L, T_T, and T_R wake center analysis performed at 1 RD, 2 RD, and 5 RD downstream (provided in a previous response) did not exhibit the opposing wake deflection signs in the upper- and lower-halves of the rotor sweep that would be expected if significant wind veer was present. To further demonstrate wind veer was not the cause of the unexpected wake skew angles, wind veer was quantified in each DD volume by analyzing the freestream wind direction profile (i.e. Fig. 5). Both the DD analysis period mean and one-sigma value of these freestream wind directions at each constant-height plane within the vertical depth of the wind turbine rotor sweep are provided in the figure below along with a time history of wind veer (defined as the freestream wind direction difference between 130 m and 30 m) in the DD analysis period. Within the DD analysis period, wind veer ranged from -4.16° per 100 m to +2.22° per 100 m about a mean value of -0.60° per 100 m. Over 80 % of the DD volumes exhibited wind veer magnitudes less than 2° per 100 m. Therefore, although wind veer can impact wake deflection, the wind veer present in the DD analysis period was not significant enough to adversely impact the results of the wake skew analysis.

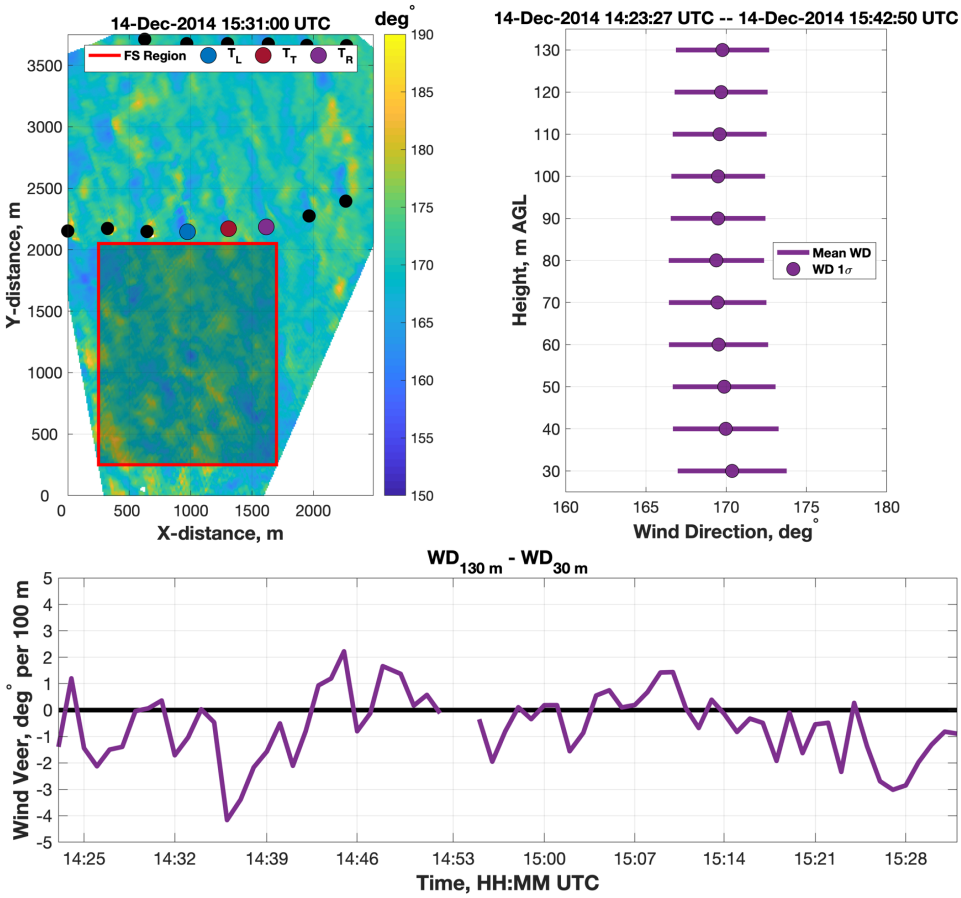

Pg. 18, ln 3: '9 degrees counterclockwise...of θ_{inf}^{V}. Stating what θ_{inf}^{V} is would clear up any confusion about the sign convention.

The value of θ_{inf}^{V} was defined in the first manuscript submission on Pg. 9 Lns. 13 through 16:

> "The freestream wind direction was defined at each DD constant-height plane within the vertical depth of the wind turbine rotor sweep (Fig. 5b), and the mean of these freestream wind direction measurements was used to determine the rotor sweep area (RSA) average turbine inflow wind direction $\left(\text{i.e. } \theta_{inf}^{V}\right)$."

However, because there is a gap in the usage of this term, manuscript text was modified to refer the reader back to Sect. 3.1.2 for the definition of θ_{inf}^{V}.

Pg. 19 Lns. 4 through 5:

> "At 15:21:08 UTC, a θ_{streak}^{V} value of 162.72° was determined, which was 9° counterclockwise (i.e. to the left when looking downstream) of θ_{inf}^{V} (defined in Sect. 3.1.2)."

Section 4.2.1: The potential impact of streak orientation on wake skew is an interesting idea. However, a deeper discussion of how this might cause the skewing of the wake would be appreciated.

In the first manuscript submission (Pg. 17, Lns. 4 through 5), it was denoted that previous research demonstrates boundary layer streak orientation can slightly deviate (i.e. clockwise or counterclockwise) from the ABL wind direction. While Lorsolo et al. (2005) is listed as the primary reference for this research, both Morrison et al. (2005) and Foster (2005) have also identified streak orientation angles that deviate from the ABL wind direction. Despite this empirical research, it is unknown why boundary layer streak orientation differs from the ABL wind direction. Rather than presenting and validating hypotheses for the formation of boundary layer streaks, previous research has commonly focused on simply quantifying the spatial and temporal structure of these boundary layer heterogeneities. However, to provide the reader with more background on this research area, the references for Morrison et al. (2005) and Foster (2005) are now provided in the manuscript.

Because the physical mechanisms that govern boundary layer streak orientation are relatively unknown, it is difficult to hypothesize how these streaks directly govern downstream wake progression. However, because the dimensions of boundary layer streaks scale well with wind turbine wakes, it can be hypothesized that the same boundary layer forcings causing streak orientation to deviate from the ABL wind direction might also promote similar deviations in wake orientation. To convey this to the reader, manuscript text was modified.

Pg. 18 Lns. 6 through 7:

> "Although it is not fully understood what causes streak orientation to differ from the ABL wind direction, it can be hypothesized that the same boundary layer forcings also promote downstream wake deviation from the ABL wind direction."

Comprehensively quantifying how boundary layer streaks modulate downstream wake progression is outside the scope of this manuscript. However, the authors hope that establishing this preliminary connection will stimulate future research that examines how boundary layer heterogeneities impact the effectiveness of various wind plant control methods.

Fig. 13: Consider showing the joint probability density of streak skew angle and wake skew angle. This would support your idea of a correlation between the two better.

Thank you for your input. A joint probability density of $\theta^{V}_{\text{S-skew}}$ versus θ^{V}_{skew} is now provided in the manuscript (i.e. Fig. 14). Corresponding to Fig. 14, the following text was incorporated into the manuscript.

Pg. 19 Lns. 11 through 15:

> "Similarities between the $\theta^{V}_{\text{S-skew}}$ and the T_L, T_T, and T_R θ^{V}_{skew} distributions are further demonstrated by examining their joint probability density. In Fig. 14 the T_L, T_T, and T_R θ^{V}_{skew} distributions were combined and compared to the $\theta^{V}_{\text{S-skew}}$ distribution; darker shades of blue indicate increasing probability of the respective $\theta^{V}_{\text{S-skew}}$ and θ^{V}_{skew} values. Despite positive values of $\theta^{V}_{\text{S-skew}}$, a large percentage of the skew angles (both $\theta^{V}_{\text{S-skew}}$ and θ^{V}_{skew})

exhibited counterclockwise rotation relative to θ_{inf}^{V} (indicating downstream deflection to the left)."

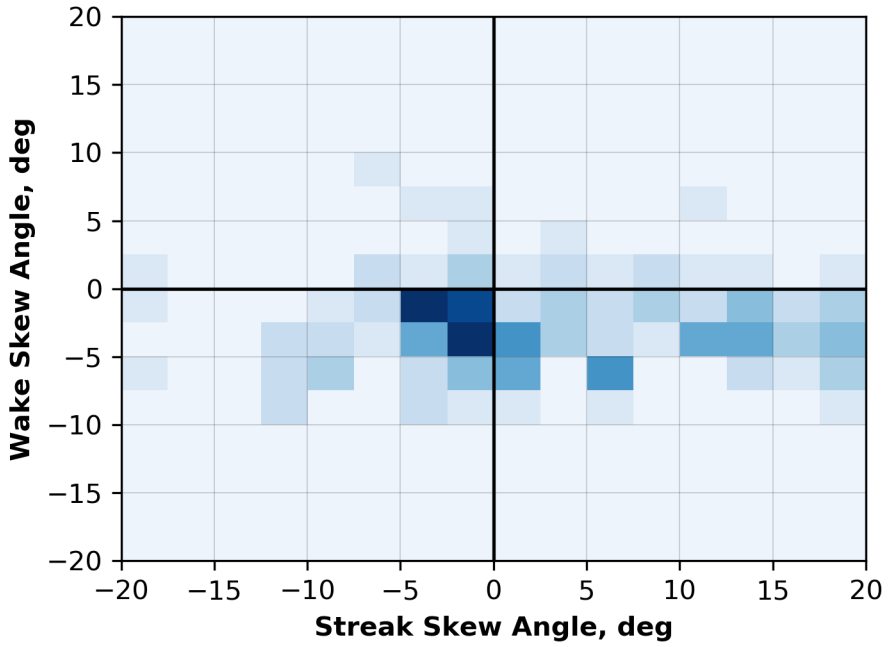

Figure 14. The joint probability density between the $\theta_{S\text{-}skew}^{V}$ and θ_{skew}^{V} distributions. The T_L, T_T, and T_R θ_{skew}^{V} distributions were combined to produce this heatmap, wherein darker shades of blue indicate an increasing probability of occurrence for the respective $\theta_{S\text{-}skew}^{V}$ and θ_{skew}^{V} values.

Section 5.1: SD WTA: For a section title, consider spelling out the acronym.

The acronym WTA is now spelled out in the section title.

Section 5: In addition to wake length and wake meandering, what differences have you observed in the relative magnitude of the velocity deficits for stable vs unstable conditions? This would be a valuable addition to the paper.

The authors agree that this would be a valuable addition to the paper. However, analysis and comparison of the convective and stable ABL wake deficit profiles was hindered by several factors. First, there were significant differences in the turbine inflow wind speed between the convective and stable ABLs (reflected in Fig. 15 [now Fig. 16] using 10-min average data). Although 10-min average wind speeds were provided in the manuscript, high-temporal resolution wind speed data spanning the SD analysis period is provided in the figure below to demonstrate these wind speed differences. The red and blue shaded regions denote the convective and stable portions of the SD acquisition period, respectively. The amount of momentum extracted from the inflow, and therefore the wake deficits immediately downstream, inversely vary as a function of the turbine inflow wind speed. Therefore, it would be difficult to exclusively attribute difference

in the convective and stable wake deficit profiles to changes in ABL stability, rather than simply differences in the turbine inflow wind speed.

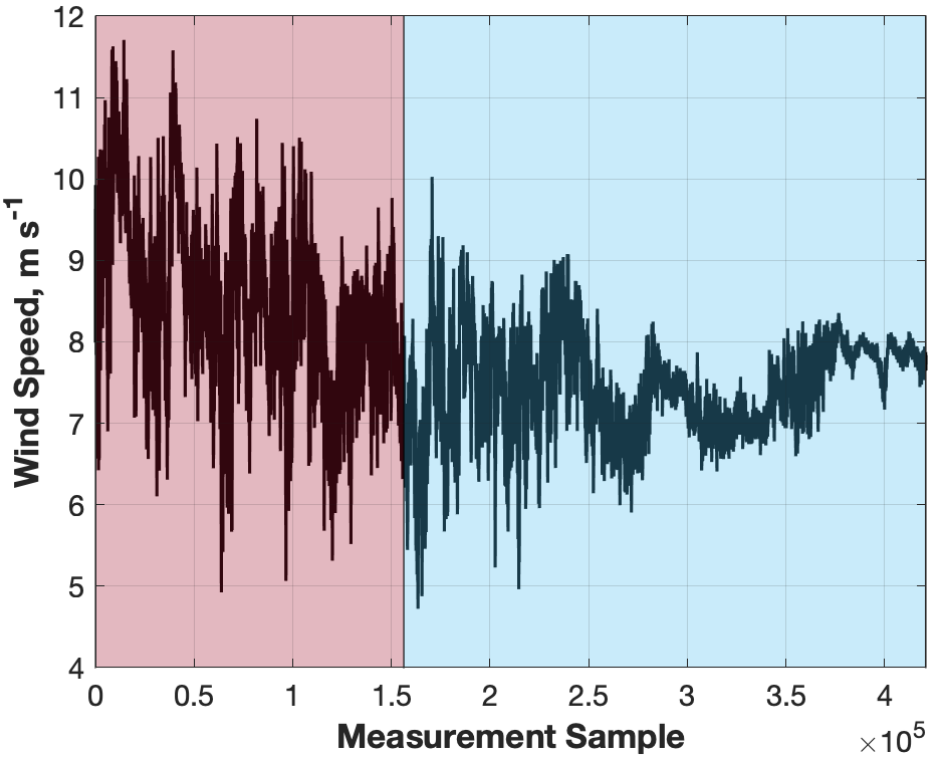

A second confounding factor to wake deficit analysis was the variation in measurement height with range (approximately 17.5 m per km moving away from the radar [noted in the manuscript on Pg. 5 Lns. 10 through 11]). This impacted the potential for wake deficit analysis as follows:

1) Wind shear varies between the convective and stable ABLs. In the stable ABL, wind shear is typically larger than in the convective ABL. Therefore, the turbine inflow wind speeds will be inherently larger than the wake velocities because of their relative measurement range and height. A shear-correction would be required to resolve relevant wake deficit profiles.

2) Because measurement height varies with range, different portions of the wake are examined at incremental distances downstream.

For these reasons, it is difficult to know how relevant the extracted wake deficit profiles would be for research purposes, or how well they would correlate with wake deficits found in previous research. Wake length was instead examined as a proxy to discern the downstream extent of the wake effect in both the convective and stable ABLs.

To more clearly convey differences in wind speed (and atmospheric turbulence) between the convective and stable ABLs, the convective and stable portions of the SD analysis period are now shaded in Fig. 15 (now Fig. 16). The revised figure was copied below for reference.

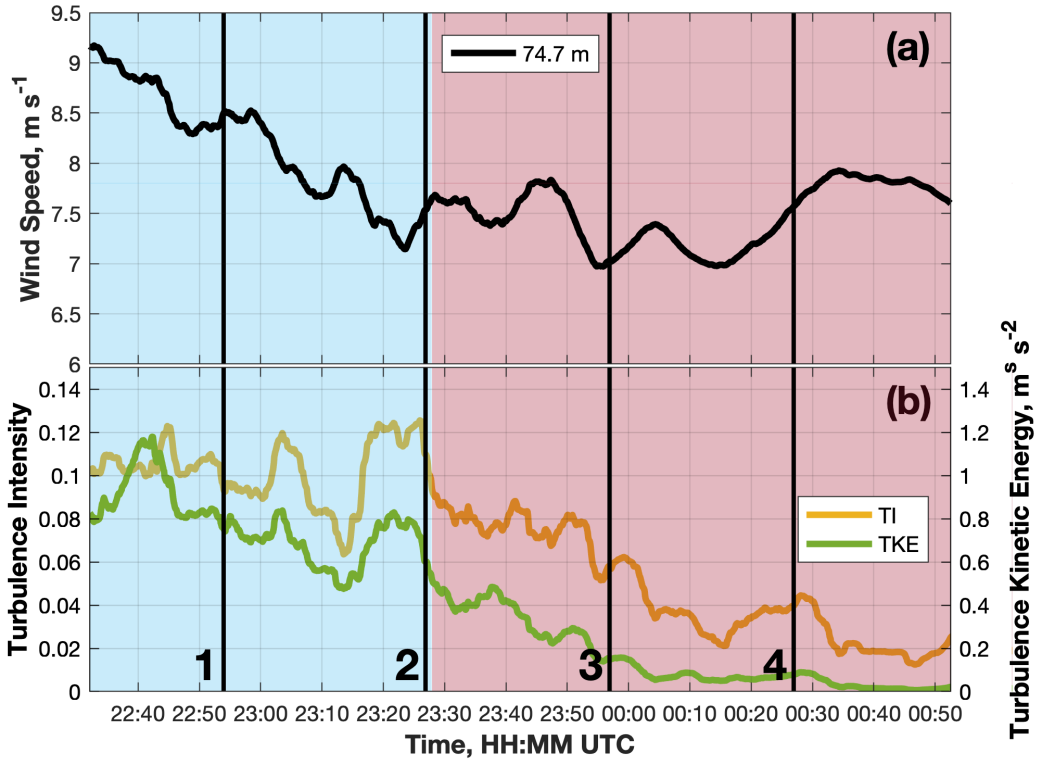

Pg. 26: ln. 14: 'access to the controller design so any factors inhibiting proper implementation of the turbine control offsets can be identified.' I agree that access to the controller improves the assessment of wind plant control strategies, and is always desirable, but I think meaningful control assessments can be done without direct access. For example, adding a pitch offset in region 2 (where pitch is typically fixed at 'fine pitch') could be achieved without needing to understand the controller dynamics. Furthermore, to implement a yaw misalignment, the yaw controller setpoint could be changed from zero to the desired offset, but full understanding of the controller dynamics is not necessary, and in many cases would be asking too much given the proprietary nature of wind turbine control systems.

Meaningful wind plant control experiments could be performed without full access to wind turbine controller design. However, a comprehensive analysis of the controller's ability to implement the desired control strategies would likely require access to its control structure and design. Without this information, it would be difficult to discern why the turbine was able/unable to implement the desired control changes and it would also be challenging to determine how these control changes could be more efficiently employed. However, manuscript text was modified to soften reader interpretation.

Pg. 28 Lns. 20 through 21:

> "...(2) access to relevant controller information (e.g. controller design) so any factors inhibiting proper implementation of the turbine control offsets can be identified."

James B Duncan Jr
https://doi.org/10.5194/wes-2019-78-RC2

General Response

Thank you for this paper. It is very useful to receive experimental results, and it is always a major undertaking to gather such data. In general the paper is well written with good and useful figures.

My major criticism/suggestion is that the results presented in sections 3/4 are of too little data, and with too many "black box" issues to be used to draw conclusions from. Section 5 on the other hand provides results which are useful, line up with physical interpretation, and show statistical significance. I would therefore propose to condense (or remove?) sections 3/4, and perhaps expand a bit on section 5.

Thank you for your comments and the time taken to provide this review. The authors are glad you appreciate the experimental data and are understanding of the difficulties inherent to data collection.

The main criticism of the referee is that the results presented in Sections 3 (Wind Plant Control Experimental Setup, Controller Assessment, and Controller Assessment Challenges) and 4 (Measuring Wind Turbine Wake Response to First-Order Turbine Control Changes) are of too little data and with too many “black box” issues to draw conclusions from. The authors agree there are innate limitations to the dataset. However, this is why the initial focus of the manuscript was modified as analyses progressed to, in part, exploring the difficulties associated with performing a wind plant control experiment at full scale.

At the time of the experiment (14 December 2014), experimental validation of wind plant control at full scale was rare. Similarly, there was a dearth of observational data (especially compared to numerical simulation) characterizing in three-dimensions wind turbine wake structure and variability. Therefore, in collaboration with an industry partner, the preliminary objectives of the experiment were to (1) examine three-dimensional wind turbine wake response to changes in wind turbine yaw and blade pitch and (2) examine how these changes impact the net power production of individual turbines in the wind plant (i.e. quantifying the effectiveness of the wind plant control strategy). However, experimental logistics (e.g. experimental control limitations imposed by the wind plant operator) ultimately inhibited the successful execution of these experimental objectives. As noted in our response to referee one, the wind plant control experiment would have been ideally performed in an environment more conducive to the effectiveness of the implemented control strategies and for longer experimental durations. Still, the authors are confident that there is value to disseminating the results of this experimental campaign, albeit in a suboptimal environment and subject to innate limitations.

The results of this study lend insight into the complexities associated with performing a wind plant control experiment at full scale, and therefore, should be used to inform future field campaigns. Section 3 provides methods that can be referenced in future studies, but furthermore, this section highlights the importance of several key data sources and how not having access to these data can severely impact both analyses potential and the ultimate success of the field campaign. Section 4 additionally establishes that strategic yaw error in some ABL environments might not be sufficient to ensure effective wake steering. The authors were not intending based off this analysis to provide

a statistical characterization of the wake. Rather, the authors are optimistic these results will promote further research examining how certain ABL conditions and transient ABL heterogeneities might impact both the effectiveness and potential benefit of various wind plant control strategies.

The results of Section 4 also provide a smooth transition to Section 5 (ABL stability driven wake changes). The referee suggests that the analysis in Section 5 should be expanded. Although this is desirable, SD wake analysis was also limited. For example, referee one advised that velocity deficits between the convective and stable ABLs be examined. However, analysis and comparison of the convective and stable ABL wake deficit profiles were hindered by several factors. First, there were significant differences in the turbine inflow wind speed between the convective and stable ABLs (reflected in Fig. 15 [now Fig. 16] using 10-min average data). Although 10-min average wind speeds were provided in the manuscript, high-temporal resolution wind speed data spanning the SD analysis period is provided in the figure below to demonstrate these differences in wind speed. The red and blue shaded regions denote the convective and stable portions of the SD acquisition period, respectively. The amount of momentum extracted from the inflow, and therefore the wake deficits immediately downstream, inversely vary as a function of the turbine inflow wind speed. Therefore, it would be difficult to exclusively attribute difference in the convective and stable wake deficit profiles to changes in ABL stability, rather than simply differences in the turbine inflow wind speed.

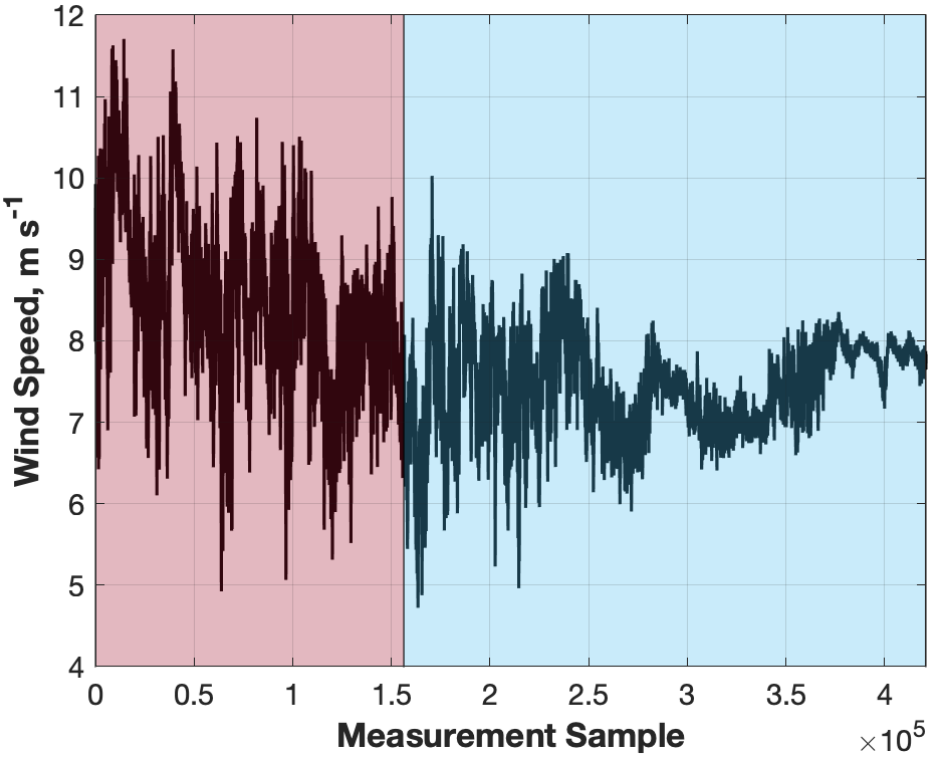

A second confounding factor to wake deficit analysis was the variation in measurement height with range (approximately 17.5 m per km moving away from the radar [noted in the manuscript on Pg. 5 Lns. 10 through 11]). This impacted the potential for wake deficit analysis as follows:

1) Wind shear varies between the convective and stable ABLs. In the stable ABL, wind shear is typically larger than in the convective ABL. Therefore, the turbine inflow wind speeds will be inherently larger than the wake velocities because of their relative measurement range and height. A shear-correction would be required to resolve relevant wake deficit profiles.

2) Because measurement height varies with range, different portions of the wake are being examined at incremental distances downstream.

For these reasons, it is difficult to know how relevant the extracted wake deficit profiles would be for research purposes, or how well they would correlate with wake deficits found in previous research. Wake length was instead examined as a proxy to discern the downstream extent of the wake effect in both the convective and stable ABLs.

Despite the inherent limitations of the datasets presented, the authors are confident they provide a valuable contribution to the scientific community by highlighting links between the ABL and wake structure and variability and how this might impact the effectiveness of wind plant control. Furthermore, exploring the difficulties associated with performing a wind plant control experiment at full scale should help improve future experimental design.

Specific Comments

P 2 "operate below their peak capacity to decrease wake effect..." this describes well static induction control, but less well wake steering and dynamic induction control

Thank you for your comment. The manuscript text was slightly modified to improve reader comprehension. The edited text is provided below.

Pg. 2 Lns. 12 through 14:

> "When wind plant control is employed, some turbines in the wind plant will modify their control settings (sometimes operating below their peak capacity) to decrease the wake effect, thereby increasing the plant-wide available kinetic energy (De-Prada-Gil et al., 2015)."

Fig 1: It's explained later, but the legend is unclear in meaning, perhaps explain more in caption

Thank you for noting that the figure was not adequately described, the other reviewer shared a similar position. As you mention, the figure was initially detailed later on in the manuscript in Section 3 (Pg. 5 Lns. 11 through 16 and Pg. 6 Lns. 1 through 2). However, upon reconsideration, the authors recognize that this text is disconnected from the description of the 14 December 2014 deployment (i.e. Section 2.1) and Fig. 1. Therefore, this text was moved to Section 2 and was slightly modified to more comprehensively describe Fig. 1. The modified text is provided below.

Pg. 4 Lns. 14 through 23:

> "Located in the DD domain of the 14 December 2014 deployment were 20 wind turbines distributed across two turbine rows. The wind turbines were characterized by a hub height of 80 m and a rotor diameter (RD) of 101 m. Supervisory control and data acquisition (SCADA) information detailing the turbine inflow wind speed (subject to the nacelle transfer function [NTF]), turbine yaw orientation, and blade pitch angle were provided at a one-hertz sampling frequency from 14:00:00 UTC to 16:59:45 UTC for seven of the wind turbines (denoted by the non-black circles in Fig. 1). Three of the seven wind turbines were located in the lead row of the wind plant (denoted by the blue, red, and purple circles in Fig. 1), while the remaining four were located in the trailing row (denoted by the white circles in Fig. 1). The three lead-row wind turbines were separated by an average distance of 1512.2 m (~15 RD) from the trailing turbine row and were laterally separated from each other by an average distance of 321.1 m (~3 RD). The wake of these three lead-row wind turbines (referred to as the T_L, T_T, and T_R) were analyzed to examine the effectiveness of the implemented wake-mitigating control strategies."

Furthermore, both the Fig. 1 caption and legend were modified to improve reader comprehension. The updated figure and revised caption are provided below.

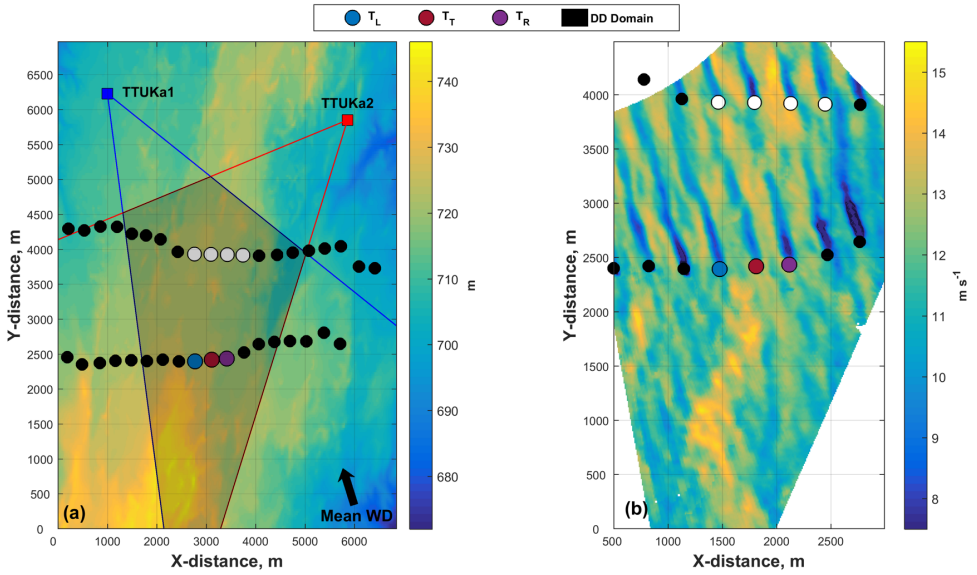

Figure 1. (a) Schematic of the TTUKa DD radar deployment on 14 December 2014 including radar deployment locations (red and blue squares), the radar sectors scanned (defined by the red and blue outlined regions), the DD domain (shaded black region), the location of the individual wind turbines (colored circles [the meaning of the different turbine colours are defined in Sect 2.1]), the mean wind direction (black arrow), and the underlying mean sea level elevation (m). (b) TTUKa DD hub-height wind speed (m s^{-1}) at 14:59:29 UTC overlaid by the wind turbine locations.

P6: RD?
RD is an acronym for rotor diameter and was established in the initial manuscript submission on Pg. 5 Lns. 12.

> "The wind turbines were characterized by a hub height of 80 m and a rotor diameter (RD) of 101 m."

This manuscript text was shifted up as part of the changes made to Fig. 1. The authors can confirm that the acronym RD was pre-established prior to its use in the manuscript.

Bottom p9: Could alternatively define wind direction as the average yaw position of non-changed turbines?

Thank you for your input. The referee suggests that wind direction could be defined as the average yaw position of non-changed turbines as opposed to using the freestream wind direction (i.e. θ_{inf}^{V}). However, the authors believe that an average wind direction based on DD measurements in the upstream 1.45 km by 1.8 km freestream analysis area is more appropriate for analyses for several reasons. One reason for opting to use θ_{inf}^{V} instead of the average yaw position of non-changed turbines is the timescales of interest in the manuscript. Wake deflection is examined on a volume-by-volume basis, or approximately at 60-s time intervals consistent with the DD volume acquisition period (i.e. 60.4 s). Therefore, to ensure the robustness of the results, the wind direction estimate used to define wake deflection should be determined at similar time intervals (i.e. $\leq$ 60.4 s). While the average yaw position of the non-changed turbines could be determined at these timescales, they are not expected to provide a more accurate estimate of the turbine inflow wind direction because of the construct of the wind turbine yaw controller. Refer to Pg. 9 Lns. 6 through 8 of the initial manuscript submission:

> "Unlike the construct of the blade pitch controller, a wind turbine will not actively yaw on a second-by-second basis to ensure optimal rotor alignment. A wind turbine will typically only yaw when the yaw error has exceeded some threshold (e.g. $\pm 10°$) for an extended period of time (e.g. 10 min)."

Therefore, as long as the yaw error does not exceed this pre-established threshold, the wind turbine will not modify its yaw to be better aligned with the inflow. While at larger timescales the wind turbine might be expected to exhibit little to no yaw error, this is not true for the minute timescales used in the presented wake deflection analysis (as demonstrated in the figure below). Provided in the top subplot is a time history of the T_L, T_T, and T_R yaw orientation angles and provided in the bottom subplot is a time history of the T_L, T_T, and T_R yaw error angles (i.e. θ_{err}^{V}) as defined relative to θ_{inf}^{V}. The vertical dashed lines denote the temporal bounds of the +10° experimental period (i.e. 15:22:00 UTC – 15:31:59 UTC). Despite the T_L, T_T, and T_R yaw controller remaining unmodified between 14:22:32 UTC and 15:22:00 UTC, each turbine exhibited significantly different yaw orientation angles. During this period wherein no turbine yaw changes were implemented, the T_L exhibited a mean yaw orientation angle of 160.6°, the T_T exhibited a mean yaw orientation angle of 156.4°, and the T_R exhibited a mean yaw orientation angle of 168.5°.

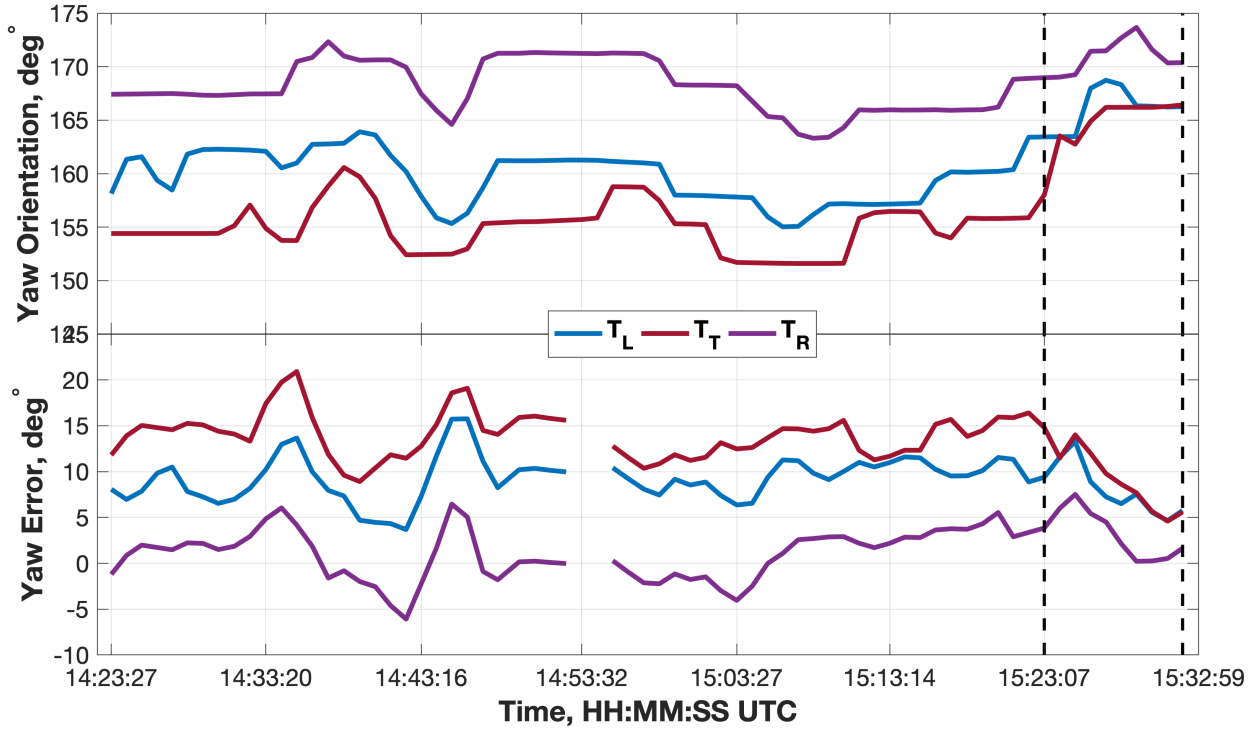

Considering each turbine exhibits yaw error (and a wide range of yaw error values at that) in this period, the authors do not believe using the average yaw position of 'non-changed' turbines is more appropriate than using θ_{inf}^{V} to define the yaw deflection angles.

Fig 8: Believe these wake directions are convex in the wrong direction, the wake deflection appears to be accelerating as heading downstream, whereas expectation would be recovery to main direction (cf fig 1 in Jiménez, Ángel, Antonio Crespo, and Emilio Migoya. "Application of a LES Technique to Characterize the Wake Deflection of a Wind Turbine in Yaw." Wind Energy, 2010. https://doi.org/10.1002/we.) this might also impact analysis in fig 10.

The referee notes that Fig. 8 indicates wake deflection increases with distance downstream. This was not the intended interpretation of the figure, instead the figure was meant to denote the general wake deflection directions (i.e. right/left) when certain yaw error angles were present (i.e. positive/negative). This is why no units were placed on either the X or Y axis. However, the authors do recognize that the reader could easily misinterpret the figure. Therefore, the figure was modified to more accurately convey the intended message. The revised figure and caption are provided below.

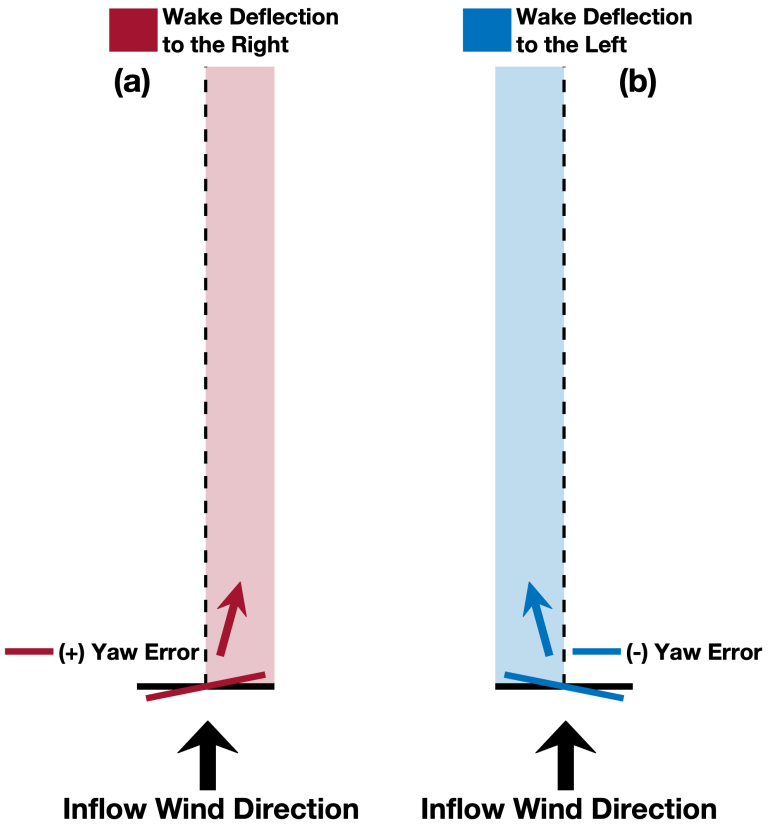

Figure 8. Wake deflection directions theoretically induced by (a) counterclockwise (i.e. $\theta_{err} > 0$) and (b) clockwise (i.e. $\theta_{err} < 0$) yaw rotation relative to a fixed turbine inflow wind direction.

The referee also correctly states that even though yaw error can promote wake deflection in a particular direction, this deflection angle will not continue infinitesimally downstream. At some downstream distance (as noted in Fig. 1 of Jiménez et al. [2010]), downstream wake progression will become more consistent with the governing wind direction. Although this is true, the authors are confident that this downstream wake behavior did not significantly impact the results presented in Fig. 10.

First, let the authors clarify that wake deflection was defined relative to θ_{inf}^{V} and not the pseudo-expected lines curves initially depicted in Fig. 8. Secondly, the aptitude of downstream wake progression to return to values consistent with the governing wind direction should slightly reduce the absolute value of the derived wake deflection angles (i.e. θ_{skew}^{V}). Therefore, had this downstream wake progression impacted results, it would also indicate that wake deflection in the near-wake region was likely more anomalous (i.e. further to the left) than that indicated by the mean T_L, T_T, and T_R values of θ_{skew}^{V}. Therefore, a return of the downstream wake progression to directions consistent with the mean flow would not have impacted the take-home message of the wake deflection analysis—the mean T_L, T_T, and T_R θ_{skew}^{V} values were opposite of that expected, indicating that some ABL characteristics (e.g. boundary layer streak orientation) might be instead governing wake orientation and downstream wake progression.

Regardless, the authors did consider the potential impact of downstream wake progression returning to directions consistent with the mean flow when performing analysis. For example, assume wake center locations outwards of only 6.5 RD downstream were considered (i.e. instead of the 13 RD used in the manuscript). Using only these wake centers to derive θ^{V}_{skew} results in the figure below (i.e. the same as Fig. 10 but using a different wake center distribution) and a mean T_L θ^{V}_{skew} value of -2.15°, a mean T_T θ^{V}_{skew} value of -2.06°, and a mean T_R θ^{V}_{skew} value of -1.27°. Therefore, these results indicate that for the downstream distances examined (i.e. 13 RD) any tendency for downstream wake progression to return to values consistent with the mean flow did not significantly impact the presented results.

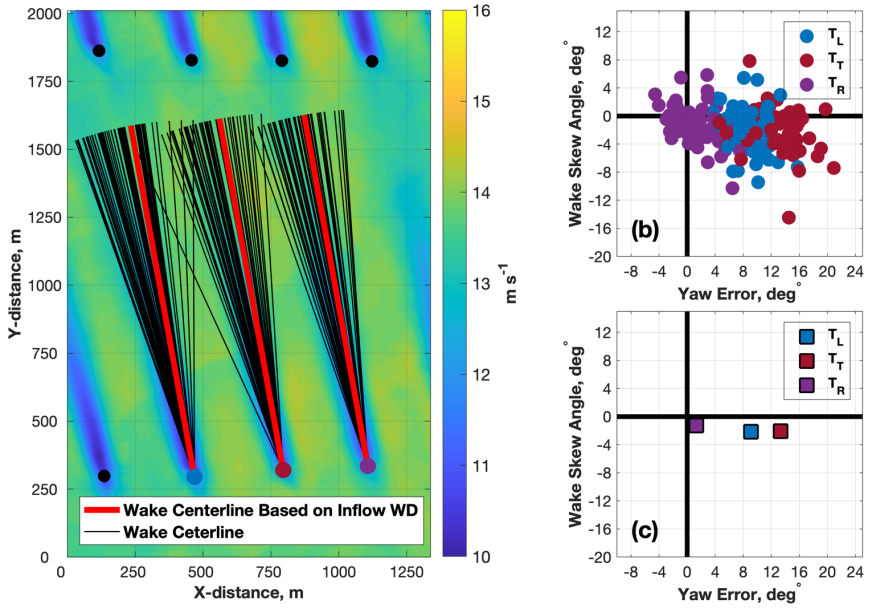

P 19 "simply implementing yaw error might not be enough to ensure effective wake steering" not clear this result can be drawn from these results

Demonstrated in the figure below, both the T_L, T_T, and T_R exhibited yaw error in the DD analysis period. The DD analysis period mean θ^{V}_{err} value was positive for each turbine (refer to Fig. 6 of the manuscript), yet the mean θ^{V}_{skew} values were negative for each turbine in the DD analysis period. These negative θ^{V}_{skew} values are opposite of expected based on theory. Therefore, positive values of θ^{V}_{err} were not sufficient given the underlying ABL conditions to elicit the expected wake deflection to the right when looking downstream.

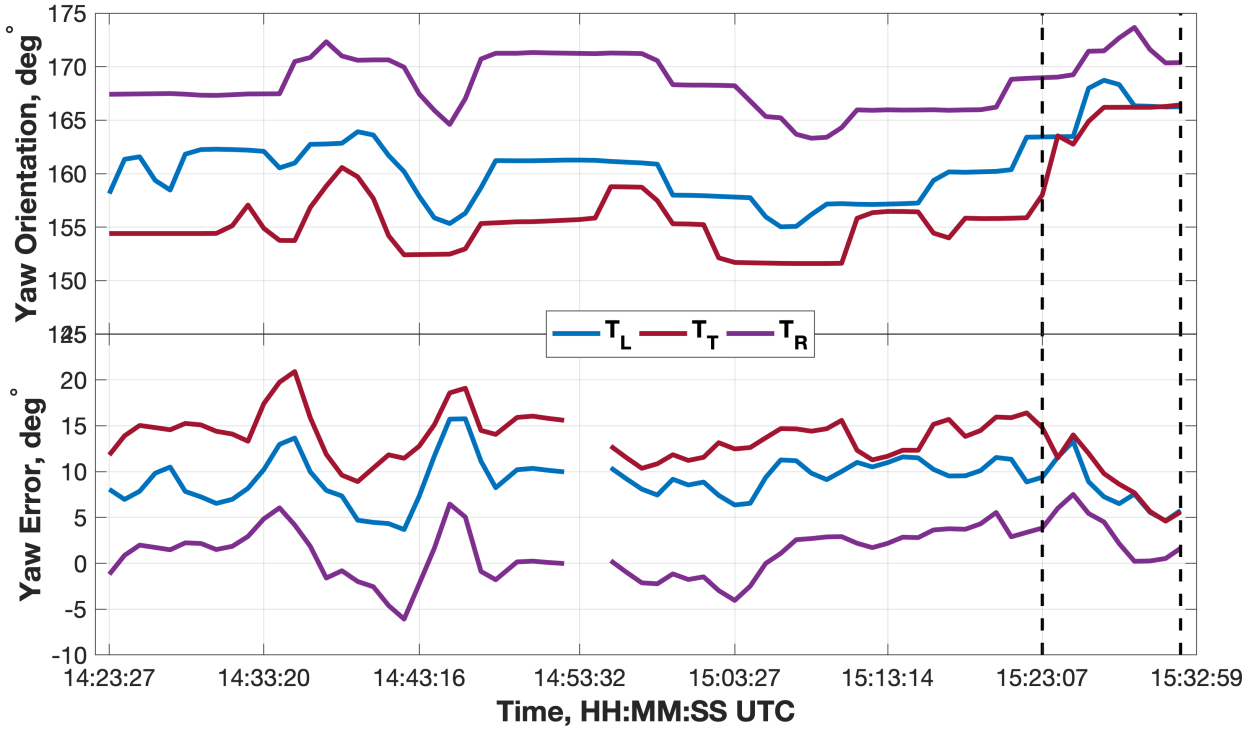

However, the authors note that the manuscript text does not adequately denote why simply implementing yaw error might not be sufficient to ensure effective wake steering. It is trivial given previous research to note that yaw-induced wake deflection is possible. However, it is not fully understood how the effectiveness of yaw-based wake steering varies given the prevailing ABL conditions. Therefore, the manuscript text was modified to indicate that in some ABLs (e.g. a convective ABL or in the presence of certain ABL heterogeneities such as ABL streaks) simply implementing yaw error might be sufficient to ensure effective wake steering.

Pg. 20 Lns. 10 through 13:

> "Regardless, these results are important because they suggest that in certain ABLs simply implementing yaw error might not be sufficient to ensure effective wake steering; rather, an integrated knowledge of ABL heterogeneities and their characteristics is needed (e.g. interaction with these transients might amplify or inhibit wake deflection)."

Fig 17 and Fig 20: Great figures and really interesting!! Text analysis also interesting

Thank you for your comment. The authors are glad that you found the analyses to be interesting.

Exploring the complexities associated with full-scale wind plant wake mitigation control experiments

James B. Duncan Jr.[1], Brian D. Hirth[1], John L. Schroeder[2]

[1]National Wind Institute, Texas Tech University, Lubbock, 79409, USA
[2]Department of Geosciences, Texas Tech University, Lubbock, 79409, USA

Correspondence to: James B. Duncan Jr. (james.b.duncan@ttu.edu)

Abstract. Recent research promotes implementing next-generation wind plant control methods to mitigate turbine-to-turbine wake effects. Numerical simulation and wind tunnel experiments have previously demonstrated the potential benefit of wind plant control for wind plant optimization, but full-scale validation of the wake-mitigating control strategies remains limited. As part of this study, the yaw and blade pitch of a utility-scale wind turbine were strategically modified for a limited time period to examine wind turbine wake response to first-order turbine control changes. Wind turbine wake response was measured using Texas Tech University's Ka-band Doppler radars and dual-Doppler scanning strategies. Results highlight some of the complexities associated with executing and analysing wind plant control at full-scale using brief experimental control periods. Some difficulties include (1) the ability to accurately implement the desired control changes, (2) identifying reliable data sources and methods to allow these control changes to be accurately quantified, and (3) attributing variations in wake structure to turbine control changes rather than a response to the underlying atmospheric conditions (e.g. boundary layer streak orientation, atmospheric stability). To better understand wake sensitivity to the underlying atmospheric conditions, wake evolution within the early-evening transition was also examined using a single-Doppler data collection approach. Analysis of both wake length and meandering during this period of transitioning atmospheric stability indicate the potential benefit and feasibility of wind plant control should be enhanced when the atmosphere is stable.

1 Introduction

During wind turbine operation, momentum is extracted from the inflow creating a waked region downstream containing less wind speed and more turbulence than the inflow (Manwell et al., 2009). When arranged in a dense array (i.e. a wind plant), wind turbine wakes can impact the performance (both power and loading) of downstream turbines (e.g. Barthelmie et al., 2007; Barthelmie and Jensen, 2010; Barthelmie et al., 2010; González-Longatt et al., 2012; Adaramola and Krogstad 2011, McKay et al., 2012; Schepers et al., 2012; Kim et al., 2015; El-Asha et al., 2017). This wake effect causes wind plant power production to be typically less than the performance of a single, stand-alone wind turbine scaled up to the number of turbines in the plant. Wake-related power losses can be significant and are heavily dependent on wind turbine spacing and atmospheric conditions,

Deleted: relative to

Deleted: be

such as wind speed, wind direction, and boundary layer stability. In the Horns Rev wind plant, wake-related power losses were estimated at 12.4% (Sørensen et al., 2006) and in the Lillgrund wind plant losses were estimated to be as high as 23% (Dahlberg and Thor, 2009). In addition, losses can be significantly higher for individual turbine pairs (e.g. upwards of 60 to 80% [El-Asha et al., 2017]). Therefore, despite innovations to wind turbine component design (e.g. improvements to the blade, generator, and tower), wake-related power losses remain a limiting factor to wind plant performance.

Wind turbine operation impacts wake structure—the more momentum extracted by the turbine, the larger the wake deficit. The controllers of individual turbines in a wind plant act autonomously, and in order to maximize power production, operate each turbine in the plant at peak capacity. However, maximizing individual turbine power extraction also increases the wake effect. Therefore, this 'greedy' control ideology is not suitable for wind plant optimization. Wind plant control (also referred to as cooperative wind turbine control or active wake control) is a next-generation control ideology designed to mitigate the wake effect (Knudsen et al., 2015). When wind plant control is employed, some turbines in the wind plant will modify their control settings (sometimes operating below their peak capacity) to decrease the wake effect, thereby increasing the plant-wide available kinetic energy (De-Prada-Gil et al., 2015). Turbine controls are typically modified to either (1) reduce wake intensity or (2) deflect the wake away from downstream turbine inflow regions (i.e. wake steering). The benefit of wind plant control has been previously demonstrated using numerical simulation (e.g. Jiménez et al., 2010; Johnson and Fritsch, 2012; Lee et al., 2013; Annoni et al., 2015; Park and Law, 2015; Fleming et al., 2015; Gebraad and van Wingerden, 2015; Gebraad et al., 2016; Park and Law, 2016; Vollmer et al., 2016; Fleming et al., 2018; Kanev et al., 2018) and in wind tunnel experiments (e.g. Parkin et al., 2001; Corten and Schaak, 2003; Howland et al., 2016; Schottler et al., 2017; Bartl et al., 2018; Bastankhah and Porté-Agel, 2019). For example, research by Park and Law (2015) indicates wind plant efficiency could be improved by 7.14 % in the Horns Rev offshore wind plant by implementing wind plant control. Despite these encouraging results, full-scale validation of wind plant control remains limited.

Experimental validation of wind plant control at full-scale has frequently relied upon the analysis of power and controls data from individual turbine pairs in a wind plant to quantify the benefit of various wind plant control techniques (e.g. Fleming et al., 2017a; Ahmad et al., 2019; van der Hoek et al., 2019; Fleming et al., 2019; Howland et al., 2019). However, few studies have used advanced measurement technologies (such as lidar or radar) to document differences in wake structure due to the turbine control changes implemented as part of wind plant control (e.g. Trujillo et al., 2016; Fleming et al., 2017b). Additionally, these studies almost exclusively limit wake measurement to the near-wake region, and therefore, are unable to monitor the downstream progression of these control-induced wake modifications. To contribute to these full-scale validation efforts, and to expand the downstream extent to which control-induced wake changes are measured, agreements were made with an industry partner to modify the yaw and blade pitch of a utility-scale wind turbine for a limited time period to examine the resulting variations in wake structure. Wake measurements were made using Texas Tech University's Ka-band (TTUKa) Doppler radars employing dual-Doppler (DD) scanning strategies. However, rather than validating the effectiveness of these

Deleted: will

Deleted: operate

Deleted: Jiménez

Deleted:

Deleted: 2010; Park et al., 2016; Vollmer et al.,

Deleted: et al., 2018; Fleming

Moved down [1]: Trujillo et al., 2016; Fleming et al.,

Deleted: 2017a; Fleming et al., 2017b;

Moved down [2]: Ahmad et al., 2019; van der Hoek et al., 2019; Fleming et al., 2019

Deleted: and measurement of wind turbine wake response to turbine control changes remains limited (e.g. Marathe et al., 2016;

Deleted:).

Moved (insertion) [2]

Moved (insertion) [1]

Deleted: To expand upon existing full-scale validation efforts

Deleted: Results

wind plant wake-mitigating control strategies, results highlight some of the complexities associated with executing and analysing wind plant control techniques at full-scale using brief experimental periods. For instance, information to accurately quantify the implementation of a control strategy is imperative to attributing the resulting variations in wake structure to the control change itself. Given wind turbine wake structure is also sensitive to the underlying atmospheric conditions and inflow variability (e.g. Barthelmie et al., 2013; Machefaux et al., 2016; Lee and Lundquist, 2017; Subramanian and Abhari, 2018), atmospheric conditions must also be simultaneously well documented and understood. To highlight wake sensitivity to atmospheric stability, and to determine how atmospheric stability impacts wind plant control efforts, onshore wake evolution within the early-evening transition (EET) was also investigated using a single-Doppler (SD) data collection approach.

Deleted: strategies

2 TTUKa radar instrumentation and deployment specifics

The TTUKa radars were used to spatially map wind plant complex flow structure and variability. These long-range scanning instruments are mobile and utilize a 0.33° half-power beamwidth, a nominal range gate spacing of 15 m, and horizontal scan speeds of 30° s^{-1} to provide high-resolution spatial measurements of the atmospheric boundary layer (ABL) winds across a region (~ 100 km^2). To resolve the horizontal structure of the flow, the azimuth of the radar scan is varied at a fixed elevation angle. A single scan made at a fixed elevation tilt is referred to as a sector scan. When only a single radar is available, a SD measurement strategy is used, and repetitive sector scans collect line-of-site velocities (i.e. the motion of the wind directly towards or away from the radar) with revisit times on the order of a few seconds. Multiple radars are used to enable DD synthesis via the collection of coordinated sector scans using multiple elevation tilts across a common area. These sector scans can then be used to construct a three-dimensional volume of the horizontal velocity vectors (i.e. the u and v wind components) within the DD domain (Lhermitte, 1971). The DD domain is defined as the region where the two radar scan regions spatially overlap and the beam crossing angles support DD synthesis (Davies-Jones, 1979). The TTUKa radars were previously shown to be an effective tool for documenting wind plant complex flow structure and variability at relevant scales of motion using both SD (Hirth et al., 2012) and DD (Hirth and Schroeder, 2013; Hirth et al., 2015; Hirth et al., 2016) data collection approaches. The technical specifications of the TTUKa radars are further detailed in Table 1 and radar deployment specifics (both performed in the US Great Plains) are provided in the subsections below.

Deleted: ,

Deleted: .

Deleted: Parameter ... [1]

2.1 14 December 2014 DD TTUKa radar deployment

The TTUKa radars were deployed to the north of an operational wind plant on 14 December 2014 to document changes in wind turbine wake structure due to both wind turbine yaw and blade pitch angle adaptations (Fig. 1a). Synchronized in time, the radars performed 50° sector scans across 14 elevation tilts angles (i.e. from 1.2° to 2.5° in intervals of 0.1°) to acquire a three-dimensional data volume in approximately one minute (60.4 s on average). A total of 70 DD volumes were collected between 14:22:32 UTC and 15:31:57 UTC (hereinafter referred to as the DD analysis period). A Barnes interpolation scheme (Barnes 1964) was used to interpolate the spatially distributed radial velocity measurements from their native polar coordinate system onto a Cartesian grid. The Cartesian grid was defined by a lateral grid spacing of 10 m and was vertically defined at

10-m intervals between 30 m and 130 m (i.e. at 10-m intervals through the vertical depth of the wind turbine rotor sweep) using a terrain-following framework. Surface elevation data (i.e. a one-arc second digital raster) from the United States Geological Survey National Elevation Dataset (http://ned.usgs.gov) was used to develop the terrain-following grid, thereby ensuring the Cartesian grid was defined at distinct constant-height intervals above-ground level (AGL). Within the DD domain (shaded region in Fig. 1a), the horizontal wind field was resolved (Fig. 1b). The DD wind maps can be interpreted as a pseudo-average of the wind conditions over the volume acquisition period, where the DD volume time stamp denotes the end of the volume period. Although in-situ meteorological measurements were not available, the presence of boundary layer streak features in the DD wind maps suggests near-neutral ABL stability (Deardorff, 1972; Lin et al., 1996; Drobinski and Foster, 2003).

Parameter	General Specification (14 December 2014 | 12 October 2015)
Peak Transmit Power	212.5 W
Transmit Frequency	35 GHz
Half-power beamwidth	0.33°
Azimuthal resolution	0.352°
Horizontal Scan Speed	30° s^{-1}
Pulse width	20 μs
Range gate spacing	15 m
Pulse repetition frequency	12 kHz | 15 kHz
Maximum range	12.5 km | 10 km

Table 1. TTUKa radar(s) technical specifications for the 14 December 2014 (DD) and 12 October 2015 (SD) radar deployments. Multiple values were provided if the technical specifications varied between the two radar deployments.

Located in the DD domain of the 14 December 2014 deployment were 20 wind turbines distributed across two turbine rows. The wind turbines were characterized by a hub height of 80 m and a rotor diameter (RD) of 101 m. Supervisory control and data acquisition (SCADA) information detailing the turbine inflow wind speed (subject to the nacelle transfer function [NTF]), turbine yaw orientation, and blade pitch angle were provided at a one-hertz sampling frequency from 14:00:00 UTC to 16:59:45 UTC for seven of the wind turbines (denoted by the non-black circles in Fig. 1). Three of the seven wind turbines were located in the lead row of the wind plant (denoted by the blue, red, and purple circles in Fig. 1), while the remaining four were located in the trailing row (denoted by the white circles in Fig. 1). The three lead-row wind turbines were separated by an average distance of 1512.2 m (~15 RD) from the trailing turbine row and were laterally separated from each other by an average distance of 321.1 m (~3 RD). The wake of these three lead-row wind turbines (referred to as the T_L, T_T, and T_R) were analyzed to examine the effectiveness of the implemented wake-mitigating control strategies.

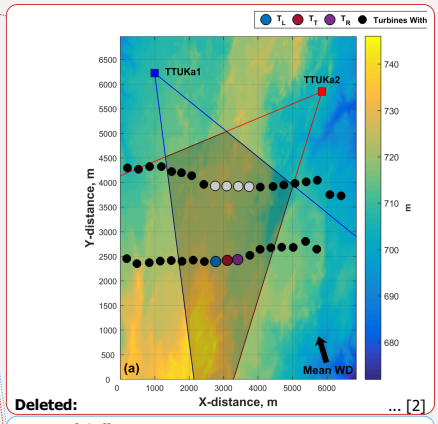

Deleted: ... [2]

Inserted Cells

Deleted: Figure 1. (a) Schematic of the TTUKa DD radar deployment on 14 December 2014 including the radar sectors scanned (red and blue lines), the DD domain (shaded region), the location of individual wind turbines (colored circles [black circles denote turbines whose SCADA data was not provided]), the mean wind direction (black arrow), and the underlying mean sea level elevation (m). (b) TTUKa DD hub-height wind speed (m s^{-1}) at 14:59:29 UTC overlaid by the wind turbine locations.

Formatted Table

Formatted: Centered, Don't add space between paragraphs of the same style, Line spacing: single

Formatted: Font: 10 pt

Moved (insertion) [3]

Moved (insertion) [4]

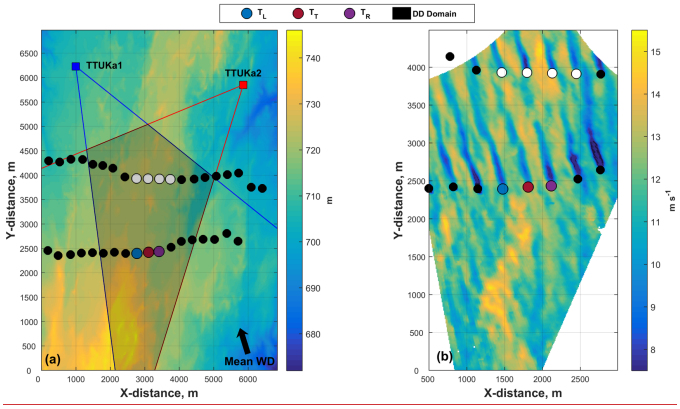

Figure 1. (a) Schematic of the TTUKa DD radar deployment on 14 December 2014 including radar deployment locations (red and blue squares), the radar sectors scanned (defined by the red and blue outlined regions), the DD domain (shaded black region), the location of the individual wind turbines (colored circles [the meaning of the different turbine colours are defined in Sect. 2.1]), the mean wind direction (black arrow), and the underlying mean sea level elevation (m). (b) TTUKa DD hub-height wind speed (m s^{-1}) at 14:59:29 UTC overlaid by the wind turbine locations.

2.2 12 October 2015 SD TTUKa radar deployment

On 12 October 2015, a single TTUKa radar was deployed to examine wind turbine wake response to changes in ABL stability consistent with the EET prevalent in the US Great Plains (Fig. 2). Between 23:32:08 UTC and 00:52:30 UTC, the radar performed a series of 1791 SD sector scans at a one-degree elevation tilt yielding an average sector revisit time of 4.7 s. Contained within the measurement domain was an instrumented meteorological tower providing wind, temperature, moisture, and pressure information at multiple vertical levels and a utility-scale wind turbine. The orientation of the scanned sector relative to the mean wind direction during the SD data acquisition period from the east-northeast allowed the wind field to be well-resolved using a SD data collection approach. A Barnes OA scheme was used to interpolate the polar radial velocity fields onto a Cartesian gridded domain with a lateral grid spacing of 20 m. However, because measurements were made at a one-degree elevation tilt, the height AGL of the gridded domain increased at a rate of 17.5 m per km moving away from the radar. The measurement height of the radar sector at the location of the wind turbine was 107.8 m AGL. This measurement height was slightly above the wind turbine hub height but within the turbine wind rotor sweep; however, further proprietary turbine information (e.g. hub height, rotor diameter) cannot be disclosed.

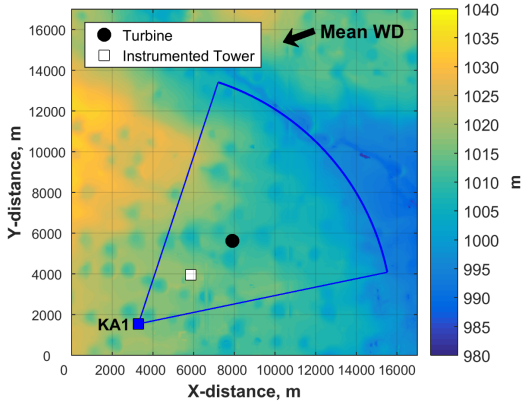

Figure 2. Schematic of the TTUKa SD radar deployment on 12 October 2015. Mapped is the underlying mean sea level elevation (m) overlaid by the location of the TTUKa radar (blue square), the radar sector scanned (blue circle arc), the mean wind direction (black arrow), the instrumented meteorological tower (white square), and the wind turbine (black circle).

Deleted: TTUKa1

3 Wind plant control experimental setup, controller assessment, and controller assessment challenges

Experimental control changes were made to a single lead-row wind turbine, referred to as the test turbine (i.e. T_T) and denoted by the red circle in Fig. 1. To examine the impact of blade pitch on wake intensity, blade pitch angle offsets of +1°, +2°, and +3° were implemented by the wind plant operator, and a +10° yaw error (positive values indicating counterclockwise rotor rotation) was employed to examine the impact of yaw error on wake deflection. Each wind turbine control change was independently implemented for a 10-min period (Table 2), meaning blade pitch and turbine yaw adaptations were not concurrently employed. Prior to analyzing wake response to wind turbine control changes, the ability of the T_T controller to accurately implement the desired control offsets was examined. The performance of the T_T controller was compared to the performance of the wind turbines to both the left (T_L) and right (T_R) of the T_T. In Fig. 1, the T_L is denoted by the blue circle and the T_R is denoted by the purple circle.

Moved up [3]: Located in the DD domain of the 14 December 2014 deployment were 20 wind turbines distributed across two turbine rows. The wind turbines were characterized by a hub height of 80 m and a rotor diameter (RD) of 101 m. Supervisory control and data acquisition (SCADA) information detailing the turbine inflow wind speed (subject to the nacelle transfer function [NTF]), turbine yaw orientation, and blade pitch angle were provided at a one-hertz sampling frequency from 14:00:00 UTC to 16:59:45 UTC for seven of the wind turbines (denoted by the non-black circles in Fig. 1).

Moved up [4]: The three lead-row wind turbines were separated by an average distance of 1512.2 m (~15 RD) from the trailing turbine row and were laterally separated from each other by an average distance of 321.1 m (~3 RD).

Deleted: Three of the seven wind turbines were located in the leading row of the wind plant, while the remaining four were located in the trailing row.

Deleted: ¶
¶

Blade Pitch Angle Offset	Time Period
+1°	14:30:00 UTC – 14:39:59 UTC
+2°	14:40:00 UTC – 14:49:59 UTC
+3°	14:50:00 UTC – 14:59:59 UTC
Yaw Error Offset	
+10°	15:22:00 UTC – 15:31:59 UTC

Table 2. Wind turbine control experiment summary for the 14 December 2014 DD deployment.

3.1 T_T controller assessment

Due to the proprietary nature of the information, wind turbine controller design was not provided by the turbine manufacturer. Not having access to wind turbine controller design is a major challenge to fully understanding wind turbine behaviour (Fleming et al., 2019), or rather, how the controller responds to variable inflow conditions when attempting to enact the desired control offsets. Therefore, the provided discussions do not detail why the turbine was able or unable to enact the desired control changes, but rather focuses on quantifying the resulting offsets. Recommendations detailing how this analysis could be improved are also provided. These recommendations can be used to inform future full-scale validation efforts.

3.1.1 Blade pitch controller assessment

The T_T is a pitch-regulated variable speed wind turbine. To achieve pitch control objectives, the pitch drive modifies blade angle of attack relative to the characteristics of the inflow. Below the rated wind speed (i.e. region two), blade pitch remains fixed to maximize turbine power extraction. Alternatively, above the rated wind speed (i.e. region three), blade pitch is actively modified according to the turbine inflow wind speed to maintain the rated generator speed and stably produce the rated power of the turbine. The benefit of modifying blade pitch for wake mitigation is expected to be greatest in region two (van der Hoek et al., 2019). Consistent with region two pitch operation, the amount of momentum extracted by the wind turbine is maximized, and therefore, wake intensity and the potential for wake-related power losses are also amplified. Furthermore, accurately implementing blade pitch angle changes might be more feasible in region two because blade pitch remains fixed (i.e. invariable of the region two turbine inflow wind speed).

Between 14:30:00 UTC and 14:59:59 UTC, the T_T was instructed to implement blade pitch angle offsets of +1°, +2°, and +3° (experimental period durations are defined in Table 2). During the experimental periods, the T_T inflow wind speeds (as defined by the nacelle anemometer) were primarily contained to region three. The T_T mean inflow wind speed was 14.26 m s^{-1} in the +1° experimental period, 14.32 m s^{-1} in the +2° experimental period, and 13.67 m s^{-1} in the +3° experimental period. Although the benefits of implementing pitch-based wake mitigation are not expected to be optimized in region three, there is still merit in examining the ability of the T_T to enact the desired blade pitch angle offsets. To maintain the rated generator speed in region three, the wind turbine follows a pitch schedule to extract the desired amount of momentum at various wind speeds. However, the pitch schedule is proprietary, and therefore, analysis of the provided SCADA information was employed to estimate it. The region three pitch schedule was constructed by fitting a linear model to the distribution of blade pitch angles as a function of the turbine inflow wind speeds. Data from all seven wind turbines with SCADA information provided (i.e. the non-black circles in Fig. 1) were used to ensure a robust estimate of the region three pitch schedule (a total of 41,343 SCADA wind speed and blade pitch angle measurements were used); measurements inconsistent with region three pitch operation and T_T data from the experimental periods were not considered when constructing the pitch schedule.

Deleted: 2018

Deleted: during

Deleted: during

Deleted: during

Deleted: benefit

The ability of the T_T controller to accurately implement the desired control offsets was quantified by comparing blade pitch angle activity within the +1°, +2°, and +3° experimental periods to the region three pitch schedule. The residual difference between the operational blade pitch angle (as defined by the SCADA) and the optimal value (as defined by the turbine inflow wind speed and the region three pitch schedule) was used to define the control change implemented. On average, the T_T exhibited a blade pitch angle offset of -0.05° during the +1° experimental period, a blade pitch angle offset of +0.68° during the +2° experimental period, and a blade pitch angle offset of -0.03° during the +3° experimental period (Fig. 3). Due to the reactive nature of the wind turbine controller, the T_T was not expected to precisely implement the desired blade pitch angle offsets on a second-by-second basis. Even so, compared to the blade pitch behaviour of the T_L and T_R (Fig. 4), wherein there were no prescribed turbine control changes, there was almost no evidence to indicate the effective implementation of distinct blade pitch angle offsets by the T_T controller in any of the experimental periods. Within the +1° and +3° experimental periods, the T_T exhibited the smallest blade pitch angle offset of all three turbines considered, and in the +2° experimental period, the T_T blade pitch angle offset was similar to that of the T_L. The mean blade pitch angle residual of the T_L, T_T, and T_R in each experimental period is provided in Table 3.

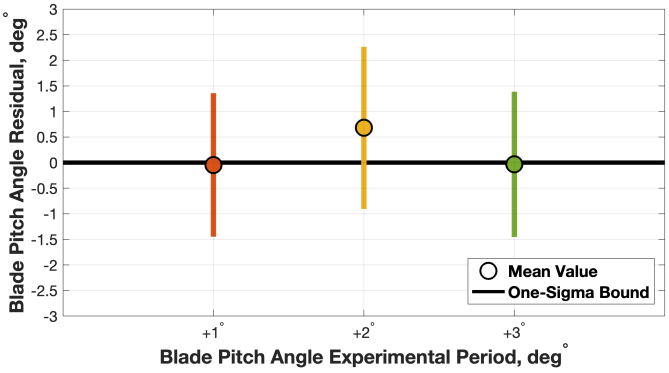

Figure 3. The mean and one standard deviation bound of the T_T blade pitch angle residual in the +1°, +2°, and +3° experimental periods.

Turbine Identifier	+1° Experimental Period	+2° Experimental Period	+3° Experimental Period	Data from all Experimental Periods
T_L	+1.03° (51.5 %)	+0.92° (86.8 %)	+1.06° (60.2 %)	+0.99° (66.2 %)
T_T	-0.05° (90.5 %)	+0.68° (90.2 %)	-0.03° (81.0 %)	+0.21° (87.2 %)
T_R	+0.20° (70.7 %)	+0.02° (86.0 %)	+0.42° (60.5 %)	+0.19° (72.4 %)

Table 3. The T_L, T_T, and T_R mean blade pitch angle residual in the +1°, +2°, and +3° experimental periods, as well as using data from all experimental periods. The values in parenthesis denote the percentage of SCADA data within each experimental period (upwards of 600 observations) that were consistent with region three pitch operation.

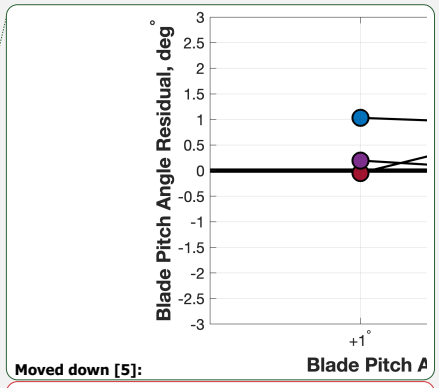

Moved down [5]:

Deleted: each

Deleted: period

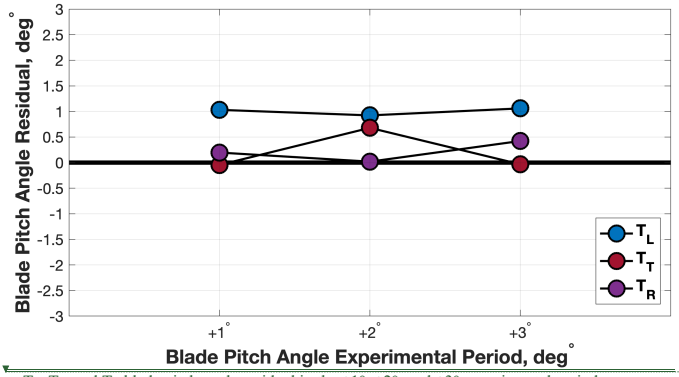

Figure 4. The mean T_L, T_T, and T_R blade pitch angle residual in the +1°, +2°, and +3° experimental periods.

3.1.2 Turbine yaw controller assessment

To ensure optimal rotor alignment, the wind turbine yaw drive orients the rotor plane roughly perpendicular to the turbine inflow wind direction (Mittelmeier and Kühn, 2018). Yaw error is defined as the misalignment angle between the rotor plane and the turbine inflow wind direction (i.e. quantifying the non-normal rotor orientation angle). Between 15:22:00 UTC and 15:31:59 UTC, the T_T controller was instructed to implement a +10° yaw error. Unlike the construct of the blade pitch controller, a wind turbine will not actively yaw on a second-by-second basis to ensure optimal rotor alignment. A wind turbine will typically only yaw when the yaw error has exceeded some threshold (e.g. ±10°) for an extended period of time (e.g. 10 min). As a result, T_T yaw error in the experimental period was expected to deviate from the prescribed +10° offset.

Although turbine yaw information was provided, turbine inflow wind direction as defined by the nacelle wind vane was not. Therefore, a freestream wind direction derived from DD radar measurements was used to estimate the turbine inflow wind direction. The freestream wind direction was defined as the mean wind direction measured across a 1.45 km by 1.8 km upstream analysis area (denoted by the red rectangle in Fig. 5a) that was free of obstacles that could impact the flow. The freestream wind direction was defined at each DD constant-height plane within the vertical depth of the wind turbine rotor sweep (Fig. 5b), and the mean of these freestream wind direction measurements was used to determine the rotor sweep area (RSA) average turbine inflow wind direction $\left(\text{i.e. } \theta_{\text{inf}}^{V}\right)$. Due to wind plant and turbine measurement limitations, yaw error is traditionally defined relative to the hub-height wind direction measured by the nacelle wind vane. However, the nacelle wind vane is unable to account for differences in wind direction with height (i.e. wind veer). Therefore, yaw error defined by the hub-height wind direction will be unable to comprehensively quantify the rotor-sweep relative variations in the axial induction

Moved (insertion) [5]

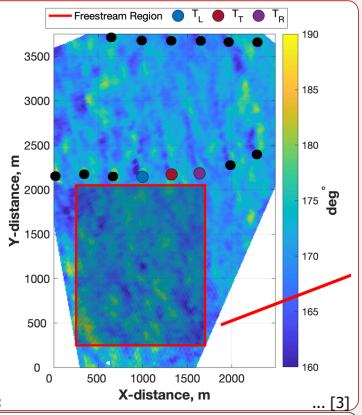

Deleted: ... [3]

Moved down [6]: Figure 5. (a) TTUKa DD hub-height wind direction (deg°) at 15:31:00 UTC overlaid by the freestream analysis area (red rectangular region). TTUKa DD wind direction measurements within the freestream analysis area were used to determine (b) the mean wind direction at each constant-height plane within the vertical depth of the wind turbine rotor sweep (i.e. the freestream wind direction profile).

factor that cause wake deflection. Hence, yaw error $\left(\text{i.e. } \theta_{\text{err}}^{V}\right)$ was defined in each DD volume relative to the RSA average turbine inflow wind direction using

$$\theta_{\text{err}}^{V} = \theta_{\text{inf}}^{V} - \theta_{\text{yaw}}^{V}, \quad 1$$

where θ_{yaw}^{V} was the DD volume yaw angle (i.e. the mean yaw angle during the DD volume acquisition period). Positive magnitudes of θ_{err}^{V} denote counterclockwise rotor rotation relative to θ_{inf}^{V}.

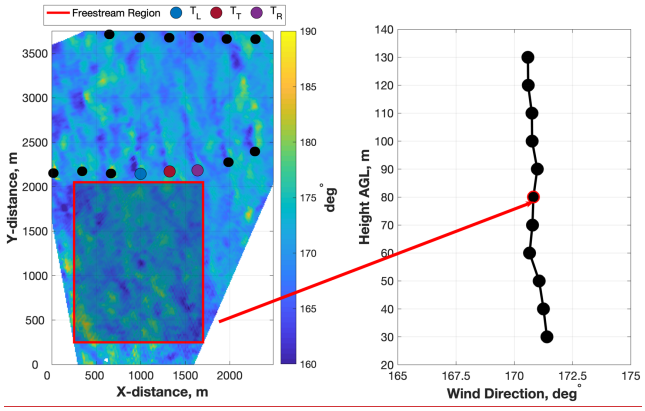

Figure 5. (a) TTUKa DD hub-height wind direction (deg°) at 15:31:00 UTC overlaid by the freestream analysis area (red rectangular region). TTUKa DD wind direction measurements within the freestream analysis area were used to determine (b) the mean wind direction at each constant-height plane within the vertical depth of the wind turbine rotor sweep (i.e. the freestream wind direction profile).

Moved (insertion) [6]

During the +10° experimental period, the T_T exhibited a mean θ_{err}^{V} value of +9.43°, a maximum θ_{err}^{V} value +14.80°, and a minimum θ_{err}^{V} value of +4.60° (Fig. 6). The T_L exhibited a similar mean θ_{err}^{V} value of +8.05° during the +10° experimental period, while the T_R exhibited a much smaller mean θ_{err}^{V} value of +3.21°. Although the mean T_T θ_{err}^{V} value was close to the desired control offset of +10°, there was insufficient evidence to indicate this value was strategic as opposed to just natural variability allowed within the construct of the wind turbine controller. Considering data from the entire DD analysis period (i.e. 14:22:32 UTC – 15:31:57 UTC), the mean T_T θ_{err}^{V} value was actually reduced (as opposed to enhanced) in the +10° experimental period. In the DD analysis period, the T_T exhibited a mean θ_{err}^{V} value of +13.32°, a maximum θ_{err}^{V} value +20.91°, and a minimum θ_{err}^{V} value of +4.60°. The T_L and T_R yaw error statistics (i.e. minimum, mean, and maximum θ_{err}^{V} values) for the entire DD analysis period are detailed in Table 4.

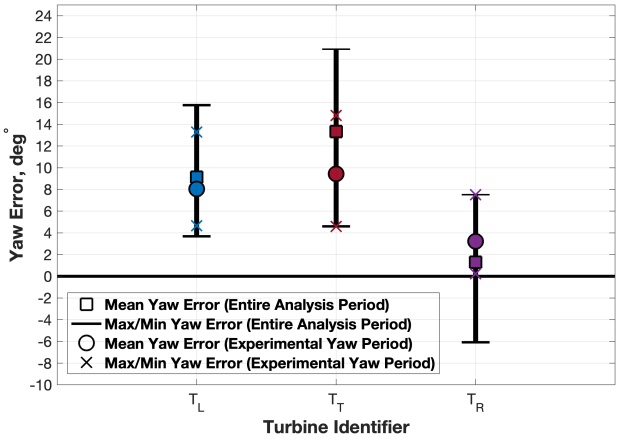

Figure 6. The mean, maximum, and minimum θ_{err}^{V} values during the +10° experimental period and the entire DD analysis period.

Turbine Identifier	+10° Experimental Period			Data from the Entire DD Analysis Period		
	Minimum	Mean	Maximum	Minimum	Mean	Maximum
T_L	+4.64°	+8.05°	13.29°	+3.68°	+9.12°	+15.76°
T_T	+4.60°	+9.43°	14.80°	+4.60°	+13.32°	+20.91°
T_R	+0.22°	+3.21°	+7.52°	-6.08°	+1.29°	+7.52°

Table 4. The T_L, T_T, and T_R minimum, mean, and maximum θ_{err}^{V} values in the +10° experimental period and within the entire DD analysis period.

3.2 Controller assessment challenges

Quantifying wind turbine control changes is imperative to determining the effectiveness of control-based wake mitigation. Being able to accurately quantify the implementation of these wake-mitigating control strategies not only lends insight into their feasibility but also increases confidence that differences in wake structure can be attributed to variations in wind turbine control. An assessment of the T_T controller was performed in Sect 3.1. Analysis determined that in each experimental period, the experimental control offsets (i.e. those realized within the individual experimental periods) were less than those prescribed to the T_T controller. Furthermore, based on comparison to the T_L and T_R, there was insufficient evidence to indicate the performance of the T_T was significantly modified by implementing the experimental control offsets. However, as detailed below, wind turbine controller assessment was limited by the data and information available and the methods used.

Deleted: ¶

Deleted: brief

The available inflow information was not optimal for controller assessment. The nacelle anemometer (subject to the NTF) was used to denote the turbine inflow wind speed and define the blade pitch angle offsets. However, nacelle-based measurements are inherently distorted due to their location behind the rotating rotor (Allik et al., 2014). Furthermore, the NTF is a proverbial black box; it is unknown what turbine signals besides the nacelle anemometer are used to produce the turbine inflow wind speed, and also unknown how well it approximates rotor-sweep relative variations in wind speed. Alternatively, area-averaged DD radar measurements were used to denote the turbine inflow wind direction and determine the yaw error. While this wind direction estimate quantifies wind veer, it is a freestream wind direction estimate, and therefore, it is does not necessarily resolve local inflow variability between the T_L, T_T, and T_R. Furthermore, this turbine inflow wind direction estimate was only available at times consistent with the DD volume acquisition period (i.e. every ~60.4 s); this limited the frequency at which wind turbine yaw error could be quantified. Consequently, neither inflow estimate provided a detailed characterization of the turbine inflow conditions at high temporal frequencies. To improve controller assessment, future field campaigns should place precedence on turbine inflow measurements (wind speed and direction) independent of the turbine control system (i.e. non-SCADA data). Experiments using scanning-based measurements should use advanced analysis techniques, such as those established in Duncan et al. (2019) wherein space-to-time conversions were performed on the spatially distributed velocity fields, to provide a comprehensive characterization of the turbine inflow wind speed and direction on a second-by-second basis. Application of these methods was limited because of data availability issues.

Deleted: (e.g.
Deleted: .,
Deleted:),
Deleted: are
Deleted: These
Deleted: were not employed herein

Wind turbine controller assessment was also hindered because controller design was not disclosed. Namely, comprehensively quantifying blade pitch control changes requires knowledge of both the region two and region three blade pitch schedules. Albeit analysis of the available SCADA information yielded an estimate of the region three pitch schedule, similar analysis was insufficient to discern the region two pitch schedule. Therefore, only region three SCADA data were considered when determining the experimental mean blade pitch angle offsets. As a result, the derived blade pitch angle offsets can only be interpreted as a best estimate of the implemented control changes. Furthermore, all that can be established without direct knowledge of the turbine controller are hypotheses detailing why the prescribed control changes were not fully implemented. For example, the brief duration of the experimental periods may have been insufficient to realize/validate the desired control offsets (in particular the ability to observe significant yaw misalignment changes), and the ability to implement the desired control changes might have been impacted by the ABL conditions present (e.g. region three inflow wind speeds). Both of these factors might have contributed to the experimental control offsets not being fully realized. However, what can be safely assumed is that the feasibility of implementing blade pitch angle changes will be improved for region two inflow, wherein blade pitch is relatively invariable of the turbine inflow wind speed.

Deleted: ,

4 Measuring wind turbine wake response to first-order turbine control changes

While the previous section details several of the challenges associated with quantifying wind turbine controller performance, some of the same inhibiting factors also limited wake analyses potential. For example, the experimental mean blade pitch angle

offsets were only considered in region three. Although a large percentage of the SCADA data in the experimental periods were consistent with region three pitch operation (refer to Table 3 for the percentages in each experimental period), the percentages between the individual turbines (i.e. the T_L, T_T, and T_R) and the experimental periods (i.e. +1°, +2°, and +3°) varied. These percentage differences make it difficult to exclusively attribute variations in wake intensity to the experimental mean blade pitch angle offsets. Furthermore, the impact of blade pitch on wake structure also depends on the characteristics of the inflow, such as the turbine inflow wind speed. Differences in the turbine inflow wind speed existed between the T_L, T_T, and T_R and the individual experimental periods (Table 5). Although individual periods could be isolated for comparison of the wake deficits relative to the blade pitch angle offset (e.g. comparing the wake of the T_T and T_R in the +2° experimental period), comprehensively quantifying the impact of blade pitch on wind turbine wake structure requires further data. Future field campaigns should implement experimental blade pitch control for longer durations to allow the effectiveness of pitch-based wake mitigation to be more comprehensively examined. Extended analysis periods will also enable averaging times sufficiently long to account for natural variability in the wake deficit profile due to turbine inflow variabilities.

Turbine Identifier	+1° Experimental Period	+2° Experimental Period	+3° Experimental Period	Data from all Experimental Periods
T_L	12.22	13.92	12.62	12.92
T_T	14.26	14.32	13.67	14.08
T_R	13.20	14.34	12.89	13.48

Table 5. The T_L, T_T, and T_R mean inflow wind speed (m s^{-1}) in the +1°, +2°, and +3° experimental periods, as well as using data from each experimental period.

Analysis was therefore limited to examining the impact of yaw error on wake deflection. Because of the brief duration of the +10° experimental period, and also because a wider range of yaw error magnitudes was available by considering data from outside the experimental periods, wake deflection analysis was performed on the entire DD analysis period (i.e. 14:22:32 UTC – 15:31:57 UTC). During the DD analysis period, the T_L exhibited a mean θ_{err}^{V} value of +9.12°, the T_T exhibited a mean θ_{err}^{V} value of +13.32°, and the T_R exhibited a mean θ_{err}^{V} value of +1.29°. Therefore, to examine the impact of larger yaw errors on wake deflection, the wake of the T_R was contrasted against the wakes of both the T_L and T_T.

4.1 DD wake-tracking algorithm

In order to examine the impact of larger yaw errors on wake deflection, a wake-tracking algorithm (WTA) established by Hirth and Schroeder (2013) was used to objectively define the wake center location at 0.25-RD intervals between 1 RD to 13 RD downstream. The WTA is detailed below and application of the WTA at 14:59:29 UTC to the wake of the T_L, T_T, and T_R is demonstrated in Fig. 7.

Deleted: from

To resolve the wake of a single wind turbine from the DD measurement volume:

1) The value of θ_{inf}^{V} (defined in Sect. 3.1.2) was used to develop a vertical wake cross-section 1 RD downstream of the turbine (denoted by the horizontal black line in Fig. 7b). The wake cross-section (characterized by a width and height of 1 RD) was oriented normal to the value of θ_{inf}^{V} and was vertically centered at hub height. The T_T wake cross-section at 14:59:29 UTC is provided in Fig. 7a.

2) At each DD constant-height plane within the wake cross-section (i.e. at 10-m intervals between 30 m and 130 m), the wind speed plane was analyzed, and the horizontal location of the wind speed minimum was determined (denoted by the red circles in Fig. 7a).

3) The median horizontal location of the wind speed minima (denoted by the red square in Fig. 7a) was defined as the wake center. Vertical wake center meandering was not considered in the WTA, and therefore, the wake was vertically centered at hub height.

4) Each subsequent wake cross-section was developed directly downwind of the previously derived wake center location. Steps 2 and 3 were repeated at each downstream distance to determine the wake center location outwards of 13 RD downstream. If the wake center location could not be determined at some distance downstream due to data availability, wake tracking for the turbine was discontinued.

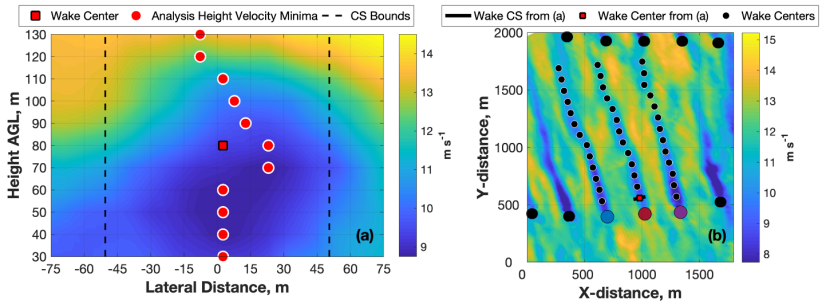

Figure 7. (a) T_T wake cross section (CS) wind speed (m s^{-1}) at 14:59:29 UTC at 1 RD downstream overlaid by the location of the wind speed minimum at each relevant analysis height (red circles) and the median horizontal location of these minima (i.e. the wake center location [denoted by the red square]). (b) TTUKa DD hub-height wind speed (m s^{-1}) at 14:59:29 UTC overlaid by the wake cross-section (black line) and wake center location (red square) from (a). Also shown at 1-RD intervals are the T_L, T_T, and T_R wake center locations (black circles).

4.2 Impact of wind turbine yaw error on downstream wake location

Assuming a uniform inflow wind direction (horizontally and vertically across the wind turbine rotor sweep), the wind turbine wake should extend directly downstream when the rotor plane is oriented perpendicular to the turbine inflow wind direction. However, when the wind turbine exhibits yaw error, wind turbine thrust will vary across the rotor plane causing the wake to be deflected, or skewed, in the direction of the rotor edge facing away from the wind (Fig. 8). Clockwise rotor rotation (i.e. $\theta_{err}<0$) relative to a fixed inflow wind direction will theoretically induce wake deflection to the left, whereas counterclockwise rotor rotation (i.e. $\theta_{err}>0$) will theoretically induce wake deflection to the right (Burton et al., 2001).

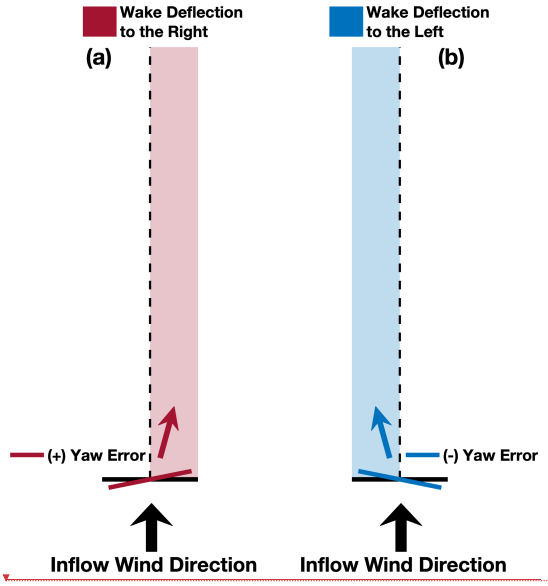

Figure 8. Wake deflection directions theoretically induced by (a) counterclockwise (i.e. $\theta_{err} > 0$) and (b) clockwise (i.e. $\theta_{err} < 0$) yaw rotation relative to a fixed turbine inflow wind direction.

To quantify wake deflection due to variations in θ_{err}, a wake skew angle was determined for each wake analyzed. The wake skew angle was defined as

$$\theta^{V}_{skew} = \theta^{V}_{wake} - \theta^{V}_{inf} \quad (2)$$

where θ^{V}_{wake} was the wake centerline angle. Constrained linear least-squares regression (Gill et al., 1981) was used to determine the value of θ^{V}_{wake}, wherein the wake centerline was required to emanate from the location of the wind turbine. The value of

Deleted: ¶

Deleted: +30° (a) -30° (b) Inflow Wind Direction Inflow Wind Direction

Deleted: (i.e. θ_{err}= +30°)

Deleted: (i.e. θ_{err}= -30°)

θ^V_{wake} minimized the error sum of squares; the error distribution was defined as the lateral distance between individual wake center locations and the wake centerline (i.e. θ^V_{wake}) (e.g. Fig. 9a). Positive values of θ^V_{skew} indicate wake deflection to the right and negative values of θ^V_{skew} indicate wake deflection to the left. Application of these methods at 15:30:00 UTC to the wake of the T_L, T_T, and T_R is provided in Fig. 9b.

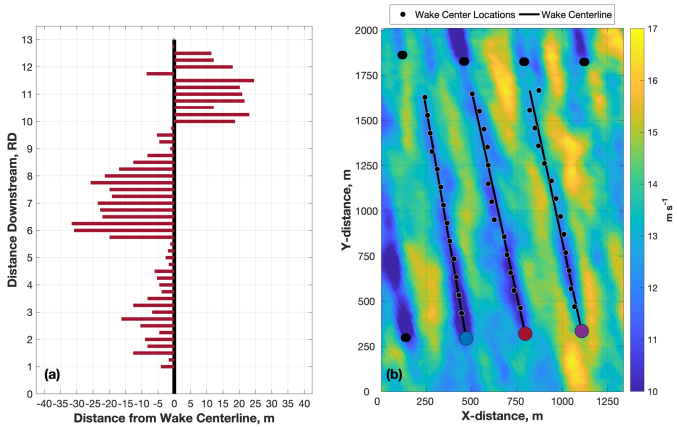

Figure 9. (a) The lateral distance between the T_T wake centerline (as defined by θ^V_{wake}) and the wake center locations (i.e. the T_T error distribution). (b) TTUKa DD hub-height wind speed (m s^{-1}) at 15:30:00 UTC overlaid by the T_L, T_T, and T_R wake centerline and the wake center locations at 1-RD increments.

Within the DD analysis period, the wakes of the T_L, T_T, and T_R were frequently skewed compared to their presumed location based on the value of θ^V_{inf} (Fig. 10a). However, the value of θ^V_{skew} did not demonstrate a strong sensitivity to the value of θ^V_{err}. Despite the T_L and T_T exhibiting larger values of θ^V_{err} than the T_R in the DD analysis period (the T_L exhibited a mean θ^V_{err} value of +9.12°, the T_T exhibited a mean θ^V_{err} value of +13.32°, and the T_R exhibited a mean θ^V_{err} value of +1.29°), all three turbines demonstrated similar magnitudes of θ^V_{skew} (Fig. 10b). The T_L exhibited a mean θ^V_{skew} value of -2.90°, the T_T exhibited a mean θ^V_{skew} value of -3.34°, and the T_R exhibited a mean θ^V_{skew} value of -2.17° (Fig. 10c). Further demonstrating the limited sensitivity of θ^V_{skew} to variations in θ^V_{err}, a linear model fit between θ^V_{skew} and θ^V_{err} exhibited a poor R^2 value of 0.18. The effectiveness of yaw-based wake steering is expected to be greater at lower wind speeds than at higher wind speeds. This is because wind turbine thrust is reduced at higher wind speeds, as are the rotor-sweep relative variations in the axial induction factor that induce wake deflection. While this can explain why θ^V_{skew} did not demonstrate a strong sensitivity to θ^V_{err}, it does not explain the average sign (i.e. $\pm$) of θ^V_{skew} in relation to θ^V_{err}. Despite on average exhibiting positive values of θ^V_{err}, the mean θ^V_{skew} value

was negative for all three turbines; indicating the observed wake deflection (i.e. to the left when looking downstream) was opposite of that expected (i.e. to the right when looking downstream). Furthermore, the values of θ^{V}_{skew} were inconsistent with θ^{V}_{inf}, which along with the weak correlation between θ^{V}_{skew} and θ^{V}_{err} provides confidence that the unexpected mean sign of θ^{V}_{skew} was not simply a result of a turbine yaw calibration error.

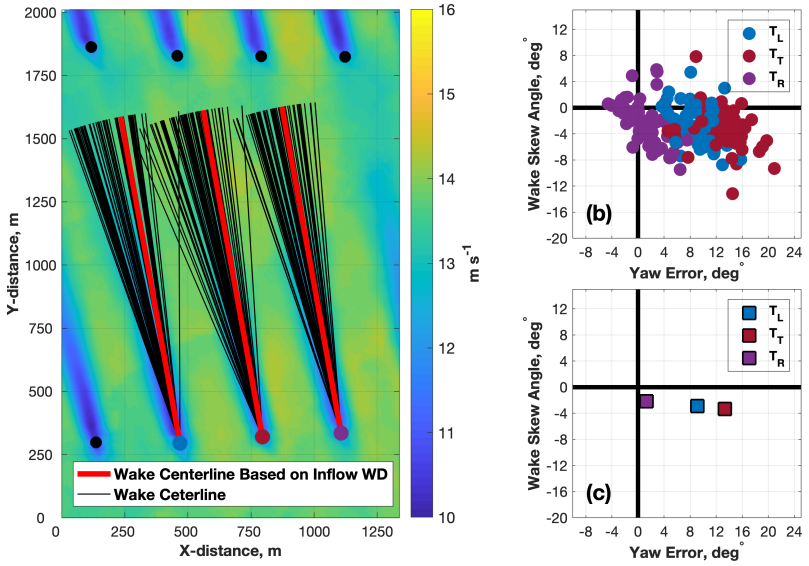

Figure 10. (a). Composite mean TTUKa DD hub-height wind speed (m s^{-1}) for the DD analysis period overlaid by the T_L, T_T, and T_R wake centerline from each contributing DD volume (black lines) and the assumed wake centerline based on the DD analysis period mean θ^{V}_{inf} value (red lines). (b) The T_L, T_T, and T_R θ^{V}_{skew} values plotted as a function of θ^{V}_{err} and (c) the turbine-respective mean values from (b).

Meteorological conditions also impact wind turbine wake structure. Although little is known how local ABL heterogeneities and other coherent turbulent structures modulate the wind turbine wake, previous research suggests downstream wake progression might be modified by transient ABL streak features (Marathe et al., 2016). Therefore, further analysis was performed to examine how ABL streaks, specifically streak orientation, might have promoted the unexpected values of θ^{V}_{skew} relative to θ^{V}_{err}.

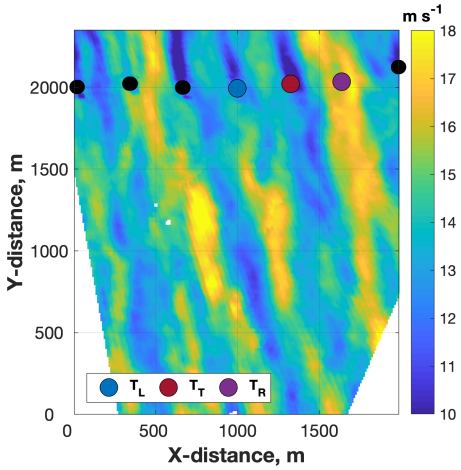

Figure 11. TTUKa DD hub-height wind speed (m s^{-1}) at 15:21:08 UTC demonstrating the presence of transient ABL streaks upstream of the lead-turbine row.

4.2.1 ABL streak orientation

Boundary layer streaks are elongated, near-surface regions of high- and low-order momentum (e.g. Fig. 11) (Drobinski and Foster, 2003; Träumner et al., 2015). Although these features are elongated in the along-wind dimension, their orientation can slightly deviate (i.e. clockwise or counterclockwise) from the ABL wind direction (Morrison et al., 2005; Foster 2005; Lorsolo et al., 2008). Although it is not fully understood what causes streak orientation to differ from the ABL wind direction, it can be hypothesized that the same boundary layer forcings also promote downstream wake deviation from the ABL wind direction.

Deleted: Lorsolo et al., 2008).

To examine ABL streak orientation and the extent to which it might have influenced θ^{V}_{skew}, a method of minimum variance (Lorsolo et al., 2008) was used to quantify streak orientation. Streak orientation was investigated at hub height in each DD volume and analysis was performed in the freestream analysis area to ensure streak orientation was not modified by the wind plant. Furthermore, to facilitate streak characterization, analysis was performed on the residual wind field to ensure the streaks were well resolved. Residual wind speeds were determined at hub height by removing from the DD wind field the freestream analysis area mean hub-height wind speed (e.g. Fig. 12a).

Streak orientation was determined at hub height in each DD volume by identifying the orientation angle that minimized variance in the residual wind field. In each DD volume, residual wind speed variance was examined across 100 transects, each 13-RD long (i.e. consistent with the search length of the WTA). These transects were orientated at 401 different angles ranging

from -20° of θ^V_{inf} to +20° of θ^V_{inf} at 0.5° intervals (Fig. 12b). The variance value assigned to each orientation angle was defined as the mean variance measured across the transects (Fig. 12c). Residual wind speed variance was assumed to be minimized in the direction parallel to the ABL streaks; therefore, the minimum variance value was used to denote the streak orientation angle $\left(\text{i.e. } \theta^V_{streak}\right)$. At 15:21:08 UTC, a θ^V_{streak} value of 162.72° was determined, which was 9° counterclockwise (i.e. to the left when looking downstream) of θ^V_{inf} (defined in Sect. 3.1.2). However, within the DD analysis period, the value of θ^V_{streak} was on average offset of θ^V_{inf} by +1.85°. The difference between θ^V_{streak} and θ^V_{inf} $\left(\text{i.e. } \theta^V_{streak} - \theta^V_{inf}\right)$ is hereinafter denoted by $\theta^V_{S\text{-}skew}$.

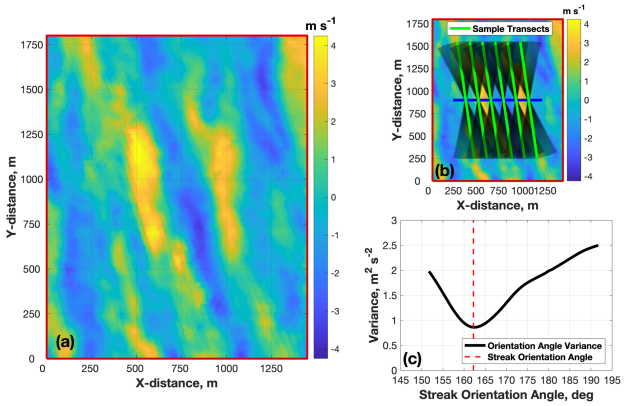

Figure 12. (a) TTUKa DD hub-height residual wind field (m s^{-1}) within the freestream analysis area at 15:21:08 UTC. (b) Same as (a) except overlaid by sample transects and the range of streak orientation angles examined (denoted by the black shaded regions). (c) The mean variance value assigned to each streak orientation angle; the minimum of this variance profile denotes the θ^V_{streak} value of 162.72° at 15:21:08 UTC.

The mean sign of $\theta^V_{S\text{-}skew}$ (i.e. +) was opposite of the turbine-respective mean θ^V_{skew} signs (i.e. -) in the DD analysis period. However, despite this difference, the peak of both the $\theta^V_{S\text{-}skew}$ and θ^V_{skew} distributions occurred between -5° and 0° (Fig. 13). Similarities between the $\theta^V_{S\text{-}skew}$ and the T_L, T_T, and T_R θ^V_{skew} distributions are further demonstrated by examining their joint probability density. In Fig. 14 the T_L, T_T, and T_R θ^V_{skew} distributions were combined and compared to the $\theta^V_{S\text{-}skew}$ distribution; darker shades of blue indicate increasing probability of the respective $\theta^V_{S\text{-}skew}$ and θ^V_{skew} values. Despite positive values of $\theta^V_{S\text{-}skew}$, a large percentage of the skew angles (both $\theta^V_{S\text{-}skew}$ and θ^V_{skew}) exhibited counterclockwise rotation relative to θ^V_{inf} (indicating downstream deflection to the left). ABL streaks were more prevalent in some DD volumes than in others, but regardless of their presence, the method of minimum variance always extracts a streak orientation angle. It is possible the

orientation angles assigned in periods of reduced streak prevalence might have impacted the mean value (and specifically the mean sign) of $\theta^V_{S\text{-}skew}$. Nevertheless, similarity in the peak of the $\theta^V_{S\text{-}skew}$ and θ^V_{skew} distributions is more noteworthy than the slight difference in the mean value of the distributions, and suggests ABL streak orientation might have contributed to the unexpected values θ^V_{skew} relative to θ^V_{err}. Furthermore, the advection direction of local ABL heterogeneities, such as ABL streaks, has previously been shown to be counterclockwise (i.e. to the left when looking downstream) of the local mean wind direction (Duncan et al., 2019).

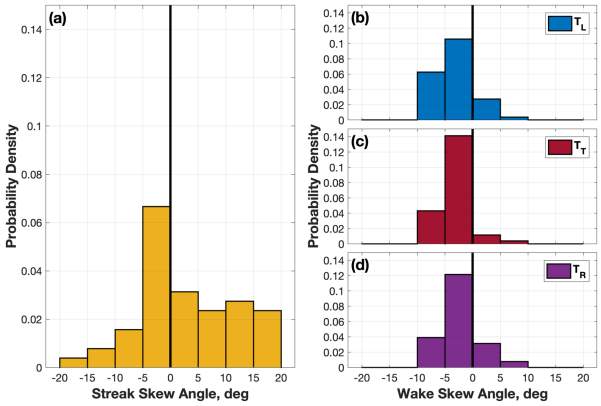

Figure 13. The probability density of the (a) $\theta^V_{S\text{-}skew}$ distribution and the (b) T_L, (c) T_T, and (d) T_R θ^V_{skew} distributions.

Although the prevalence of ABL streaks might have contributed to the ineffectiveness of yaw-based wake steering, there was insufficient evidence to conclude they are the root cause of the mean sign of θ^V_{skew}. Regardless, these results are important because they suggest that in certain ABLs simply implementing yaw error might not be sufficient to ensure effective wake steering; rather, an integrated knowledge of ABL heterogeneities and their characteristics is needed (e.g. interaction with these transients might amplify or inhibit wake deflection). These results demonstrate the importance of research that examines the impact of transient ABL heterogeneities and coherent turbulent structures on wind turbine wake structure and variability. This information is needed to optimize wind plant control.

Deleted: enough

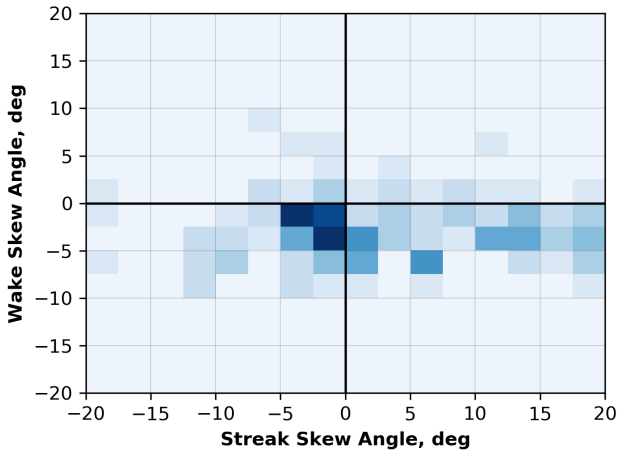

Figure 14. The joint probability density between the $\theta^{V}_{S\text{-}skew}$ and θ^{V}_{skew} distributions. The T_L, T_T, and T_R θ^{V}_{skew} distributions were combined to produce this heatmap, wherein darker shades of blue indicate an increasing probability of occurrence for the respective $\theta^{V}_{S\text{-}skew}$ and θ^{V}_{skew} values.

5 ABL stability driven wake changes

To better understand wind turbine wake response to changes in the ABL, and how this might impact the effectiveness of control-based wake mitigation, wind turbine wake evolution (i.e. wake length and meandering) within the EET was examined. The EET denotes the transition between the daytime convective and nocturnal stable ABLs. This evolutionary period of atmospheric stability is consistent with distinct changes in wind speed, wind direction, wind structure, atmospheric turbulence, and temperature (Mahrt, 1981; Nieuwstadt and Brost, 1986; Acevedo and Fitzjarrald, 2001; Edwards et al., 2006). To track the progression of the EET and the onset of the nocturnal stable ABL, the virtual potential temperature (i.e. θ_v) gradient between 10 m and 200 m was examined using available meteorological tower data. The gradient in θ_v gives an indication of how conducive the ABL is towards the development of turbulent eddies, and therefore, can be used to discern atmospheric stability. The ABL was defined as stable when the θ_v gradient was positive and was defined as unstable when the θ_v gradient was negative. The θ_v gradient was determined for each SD sector scan by analyzing thermal measurement from a 10-min period that was temporally centered on the sector scan completion time (i.e. the scan-centric analysis period). Using these

scan-centric θ_v gradient values, the convective ABL lasted from the start of data collection (22:32:08 UTC) to 23:27:53 UTC, and the stable ABL persisted until the conclusion of data collection (00:52:30 UTC) (Fig. 15).

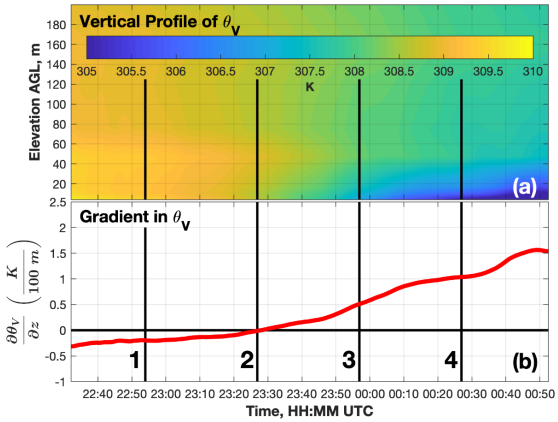

Figure 15. Evolution during the SD data acquisition period of the scan-centric (a) θ_v vertical profile (K) and (b) the θ_v gradient (K per 100 m). The magnitude of the θ_v gradient at the times consistent with the numerically labelled vertical black lines is provide in Table 6.

Wind characteristics evolved with the progression of the EET. Mean wind speeds derived from the scan-centric analysis periods at the 74.7 m meteorological tower level were strongest (i.e. exhibiting a mean value of 8.16 m s^{-1}) in the convective ABL before steadily decreasing in magnitude to a mean value of 7.48 m s^{-1} in the nocturnal stable ABL (Fig. 16a). To characterize changes in the intensity of atmospheric turbulence, trends in both turbulence intensity (TI) and turbulence kinetic energy (TKE) were examined (Fig. 16b). TI was defined as the ratio between the mean (μ) and standard deviation (σ) $\left(\text{i.e. } \frac{\sigma}{\mu}\right)$ of wind speed measurements made within the individual scan-centric analysis periods, and TKE was defined as $0.5\left(\sigma_u^2+\sigma_v^2+\sigma_w^2\right)$ where σ with subscripts u, v, and w denote the standard deviation of the along-wind, lateral, and vertical wind field components, respectively. Both TI and TKE exhibited their peak values in the convective ABL before decreasing in magnitude with the progression of the nocturnal stable ABL. Values of the θ_v gradient, mean wind speed, TI, and TKE at various times within the SD analysis period (denoted by the numerically labelled black lines in Figs. 14 and 15) are provided in Table 6. Measurements at 74.7 m AGL were analyzed because of their proximity to the wind turbine hub height.

Deleted: 14

Deleted: 14

Deleted: 15a

Deleted: 15b

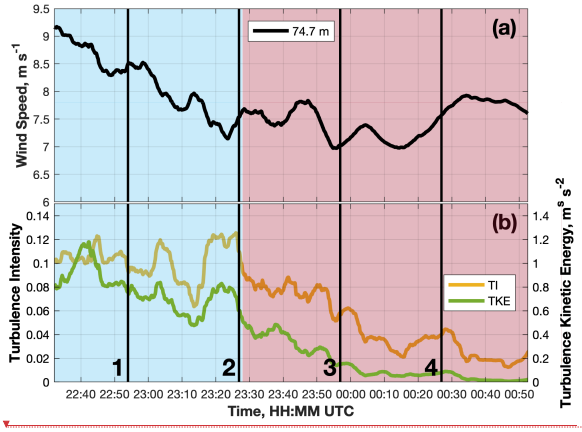

Figure 16. Evolution during the SD data acquisition period of the scan-centric (a) mean wind speed (m s^{-1}) and (b) both TI and TKE at 74.7 m AGL. The scan-centric mean wind speed, TI, and TKE values at the times consistent with the numerically labelled vertical black lines are provided in Table 6. The red and blue shaded regions denote the convective and stable portions of the SD data acquisition period, respectively.

ABL Stability and Turbulence Parameters	(1) 22:53:57 UTC	(2) 23:26:53 UTC	(3) 23:56:54 UTC	(4) 00:26:56 UTC
θ_v Gradient (K per 100 m)	-0.20	-0.01	0.51	1.04
Wind Speed (m s^{-1})	8.50	7.54	7.03	7.57
TI	0.09	0.11	0.06	0.04
TKE (m^2 s^{-2})	0.76	0.60	0.15	0.08

Table 6. 12 October 2015 SD deployment ABL characterization summary. Provided at (1) 22:53:57 UTC, (2) 23:26:53 UTC, (3) 23:56:54 UTC, and (4) 00:26:56 UTC (i.e. corresponding to the numerically labelled vertical black lines in Figs. 15 and 16) is the θ_v gradient and at 74.7 m AGL the mean wind speed, TI, and TKE.

5.1 SD wake-tracking algorithm

Slight modifications were made to the DD WTA to accommodate SD measurement of the wind turbine wake. These modifications are detailed below.

1) Because SD sector scans were performed at a one-degree elevation tilt, analysis of the vertical wake structure at incremental distances downstream was not possible. The SD wake cross-sections were instead developed along the sloped 2D plane (i.e. roughly defined for a single height AGL at each distance downstream) and the wake center

Deleted:

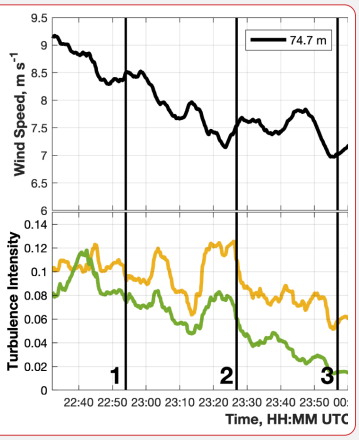

Deleted: 15

Deleted: 14

Deleted: 15

Deleted: *WTA*

location was defined as the horizontal location of the wake cross-section wind speed minimum. However, to facilitate derivation of wake length (defined in Sect. 5.2), the width of the wake cross-section was increased to 200 m.

2) SD measurements do not resolve wind direction. Therefore, both the downstream bearing and normal orientation of the wake cross-sections were defined by a 60-s scan-centric (i.e. ±30 s of the sector scan completion time) average wind direction derived using tower measurements at 74.7 m AGL.

3) Because the wind turbine RD cannot be disclosed, the WTA was not applied at RD-normalized increments (i.e. 1 RD, 1.25 RD, etc.), but instead was applied at 50-m intervals between 150 m and 3200 m downstream.

Application of the SD WTA to the wind turbine wake at 22:38:25 UTC is provided in Fig. 17a.

Deleted: 16a

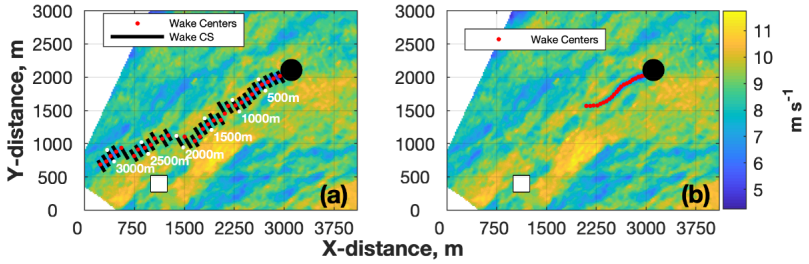

Figure 17. (a) The WTA applied to the TTUKa radial velocity wind field (m s^{-1}) at 22:38:25 UTC overlaid by the location of the instrumented meteorological tower (white square) and the wind turbine (black circle). Also plotted at 100-m intervals are the individual wake cross-sections (black lines) and wake center locations (red circles). (b) Valid wake center locations after applying the wake cessation criteria.

Deleted: 16

5.2 Wake length

The size and intensity of turbulent eddies impact the rate at which the wake-adjacent wind field (i.e. the freestream) is mixed into the wake. Variations in the magnitude of turbulence-induced mixing between the convective and stable ABLs should cause wake length to grow with the onset and progression of the EET. However, the WTA does not differentiate between wake and non-wake (e.g. transient lull features) velocity minima. Provided adequate data availability, wake center locations were always defined to a downstream distance of 3200 m. To discern wake cessation, the lateral shift between successive wake center locations, defined as the distance between the actual and projected wake center location, was analyzed. Wake cessation was defined as the downstream distance where the lateral shift between successive wake center locations exceeded 50 m. The

objective when developing these methods was to discern trends in wake length. Therefore, these values should be interpreted as robust estimates rather than exact measures of wake length. Application of these methods at 22:38:25 UTC produced a wake length of 1000 m (Fig. 17b).

Deleted: 16b

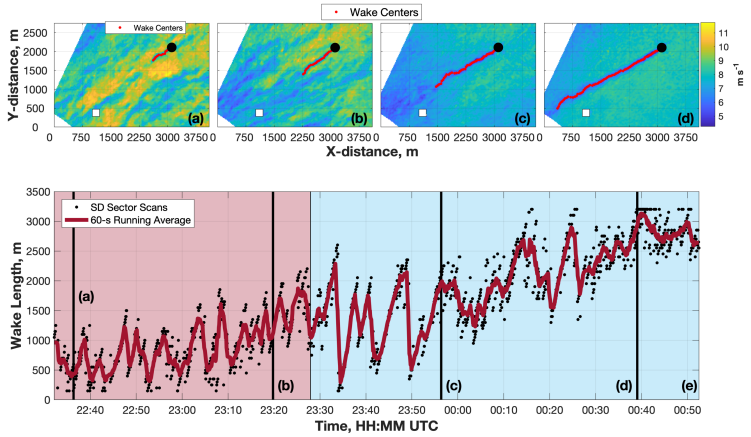

Figure 18. The TTUKa radial velocity wind field (m s^{-1}) at (a) 22:36:21 UTC, (b) 23:19:46 UTC, (c) 23:56:23 UTC, and (d) 00:39:04 UTC overlaid by the location(s) of the instrumented meteorological tower (white square), the wind turbine (black circle), and the WTA-derived wake centers (red circles). (e) Wake length time history overlaid by a 60-s running average of wake length; the red and blue shaded regions denote the convective and stable portions of the SD data acquisition period, respectively.

Deleted: 17

Clear variations in wake length existed between the convective (e.g. at 22:36:21 UTC [Fig. 18a] and 23:19:46 UTC [Fig. 18b]) and stable (e.g. at 23:56:23 UTC [Fig. 18c] and 00:39:04 UTC [Fig. 18d]) ABLs. In the convective ABL, wake length fluctuated between 150 m (i.e. the lowest detectable wake length) and 2200 m about a mean value of 907 m. The prevalence of turbulent transients in the convective ABL likely impacted the ability of the turbine to continuously impart optimal thrust, and therefore, contributed to the absence of a persistent downstream wake. As the EET progressed and ABL stability increased, wake length began to grow. However, this trend was not steady, rather large and temporally sharp changes in wake length occurred (Fig. 18e) at times. For example, at 22:33:50 UTC a portion of the wake became 'detached' from the turbine (Fig. 19a). The detached wake feature advected downstream in subsequent sector scans allowing a new contiguous wake to form (Fig. 19b). Similar wake discontinuities occurred at 23:38:13 UTC, 23:41:00 UTC, and 23:49:01 UTC. These discontinuities can be attributed to suboptimal wind turbine thrust and demonstrate the importance of wake analyses at smaller time scales. Much of this variability would be lost if the measurement periods were increased and/or the analysis was averaged

Deleted: 17a
Deleted: 17b
Deleted: 17c
Deleted: 17d
Deleted: 17e
Deleted: 18a
Deleted: 18b

across longer time frames. Despite these discontinuities, wake length increased by an average of 115.92 % between the convective and stable ABLs.

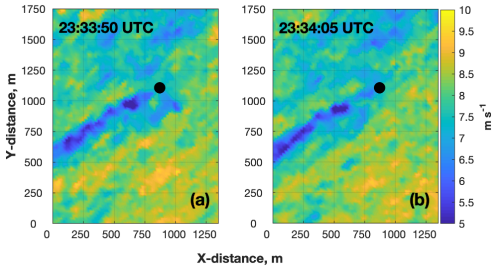

Figure 19. The TTUKa radial velocity wind field (m s^{-1}) at (a) 23:33:50 UTC and (b) 23:34:05 UTC demonstrating wake discontinuities.

Deleted: 18

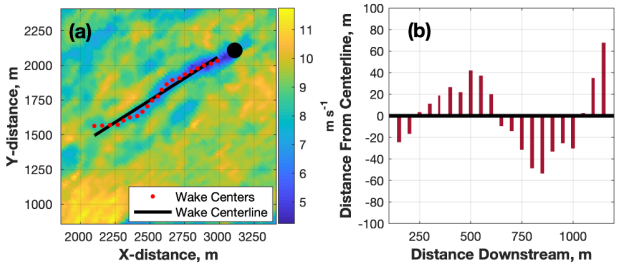

Figure 20. (a) The TTUKa radial velocity wind field (m s^{-1}) at 22:38:25 UTC overlaid by the wind turbine (black circle), the wake centerline (black line), and the individual wake center locations (red circles). (b) Vertical red lines denote the lateral deviation (m) of the wake centers from the wake centerline.

Formatted: Font: Italic

Formatted: Don't add space between paragraphs of the same style

5.3 Wake meandering

Wake meandering is the oscillating behaviour of the wake in both the horizontal and vertical dimensions of the atmosphere as it advects downstream. Wake center variability about the wake centreline was analyzed to discern variations in wake meandering consistent with the onset and progression of the EET. However, only horizontal wake meandering was considered because the SD strategies exclusively provided measurements along a single sloped 2D plane. Linear regression was used to determine the wake centerline, albeit for this analysis the wake centerline was not required to emanate from the location of the wind turbine (Fig. 20a). The mean (μ) and standard deviation (σ) of the wake center variability (i.e. lateral variability about the wake centreline [e.g. Fig. 20b]) was used to quantify horizontal wake center meandering at incremental distances

Deleted: 19a

Deleted: 19b

downstream. Horizontal wake center meandering statistics (i.e. $\mu \pm 1\sigma$) are provided in Fig. 21 as a function of ABL stability. Statistics were only plotted for downstream distances where at least 50 wake centers were derived (wake centers downstream of the wake cessation point were not analyzed).

The σ value of horizontal wake center meandering was amplified in the convective ABL. For downstream distances where wake meandering statistics were defined for both the convective and stable ABLs (i.e. from 150 m to 1600 m), σ_{stable} was on average 37.55% smaller than $\sigma_{convective}$, and at no common distance downstream was σ_{stable} greater than $\sigma_{convective}$. In both the convective and stable ABLs, the value of σ initially decreased with distance downstream (until approximately 500 m) before steadily increasing in magnitude. Despite this initial decrease, which might be due to deepening velocity deficits, the value of $\sigma_{convective}$ increased by 82.02% from a mean value of 25.64 m at 150 m downstream to a mean value of 46.67 m at 1000 m downstream. Alternatively, only a 27.80% increase was noted between these two distances in the stable ABL.

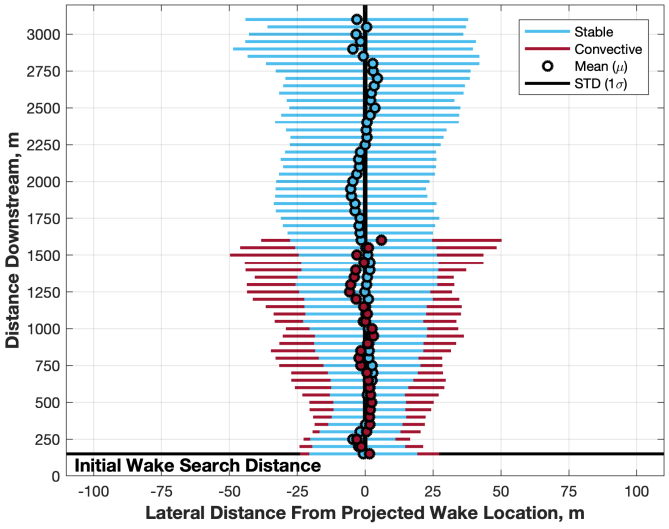

Figure 21. Horizontal wake center meandering mean values (colored circle) and one standard deviation bounds (colored horizontal line) as a function of distance downstream (the plotted colours reflect the ABL stability classification).

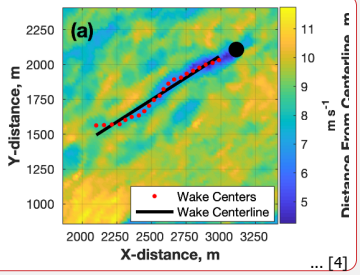

Deleted: 20

Deleted: ... [4]

Deleted: 20

Deleted: colors

6 Concluding remarks

Wake measurements were made using the TTUKa radars to examine the effectiveness of two wake-mitigating control strategies at full-scale. However, instead of validating these wind plant control methods, results highlighted some of the complexities associated with executing and analysing wind plant control at full-scale using brief experimental control periods. Some difficulties include (1) the ability to accurately implement the desired control changes, (2) identifying reliable data sources and methods to allow these control changes to be accurately quantified, and (3) attributing variations in wake structure to turbine control changes rather than a response to the underlying atmospheric conditions (e.g. boundary layer streak orientation, atmospheric stability).

Modifications were made to the yaw and blade pitch of a utility-scale wind turbine (i.e. the T_T) in this study to examine how control changes impact wind turbine wake structure and downstream progression. However, despite instructing the T_T controller to implement distinct blade pitch angle and turbine yaw offsets, in each experimental period the observed control offsets were less than those prescribed. Furthermore, based on comparison to the T_L and T_R, there was insufficient evidence to indicate the performance of the T_T was significantly modified by implementing the experimental control offsets. These results indicate a reactive wind turbine controller might struggle to accurately implement turbine control offsets, at least for the time scales (i.e. 10 min) and wind speeds (i.e. region three) examined. However, wind turbine controller assessment was limited; the available inflow information was not optimal for controller assessment and without direct access to controller design, it was impossible to determine why the control offsets were not fully realized. Based off these results, comprehensive controller assessment requires (1) a data source providing near-continuous, and reliable (i.e. accurate) turbine inflow information, and (2) access to relevant controller information (e.g. controller design) so any factors inhibiting proper implementation of the turbine control offsets can be identified. However, if this information cannot be secured, the presented methods can be used as a reference guide for controller assessment.

Because of experimental difficulties, analysis of wind turbine wake response to turbine control changes was limited to examining the impact of yaw error on wake deflection. The wakes of the T_L, T_T, and T_R were frequently skewed compared to their presumed location based on the value of θ^V_{inf}. The mean direction of θ^V_{skew} for all three turbines (i.e. to the left when looking downstream) was opposite of that expected (i.e. to the right looking downstream) based on the values of θ^V_{err}. To examine whether local boundary layer transients such as ABL streaks might be modifying downstream wake progression, ABL streak orientation was quantified and compared to θ^V_{skew}. Although the mean value of $\theta^V_{S\text{-}skew}$ $\left(\text{i.e. } \theta^V_{streak} - \theta^V_{inf}\right)$ was different than the turbine-respective θ^V_{skew} values, the peak of both the $\theta^V_{S\text{-}skew}$ and turbine θ^V_{skew} distributions was between -5° and 0°, which suggests ABL streak orientation might have contributed to the unexpected values θ^V_{skew} relative to θ^V_{err}. This result is important because it indicates proactively implementing yaw error might not be sufficient to ensure effective wake steering without at least an integrated knowledge of ABL heterogeneities and their characteristics.

To further examine how atmospheric conditions might impact the effectiveness of wind plant control, wind turbine wake evolution within the EET was examined. Between the convective and stable ABLs, mean wake length increased by 115.92%, indicating the likelihood of negative turbine-to-turbine wake interaction will be amplified in the stable ABL. Furthermore, the σ value of horizontal wake center meandering was reduced by 36.55 % in the stable ABL. This reduction in σ indicates the downstream deterministic location of the wake should be increased in the stable ABL, which should also increase the effectiveness of control-based wake modulation (e.g. wake steering). These results are significant and suggest the potential benefit and feasibility of wind plant control should be increased in the stable ABL, where both the potential for wake-related power losses and the ability to modify the wake should be amplified. In other ABL environments, local ABL heterogeneities might govern wake structure, variability, and downstream progression. More research is needed to understand how, in addition to turbine controls, transient ABL heterogeneities impact and govern wind turbine wakes. This information is fundamental to optimizing wind plant control.

Data availability

The data are not publicly available because of the agreed upon non-disclosure agreements with the turbine manufacturer.

Author contributions

James Duncan, Brian Hirth, and John Schroeder contributed to the design and execution of the two radar deployments. Data analyses were performed by James Duncan under the supervision of both Brian Hirth and John Schroeder. The manuscript was prepared by James Duncan and reviewed by both Brian Hirth and John Schroeder.

Competing interests

The authors do not have any competing conflicts of interest.

Acknowledgements

Funding for this study was provided by the National Science Foundation award CBET-1336935. The authors also thank Dr. Richard Krupar III for assistance with the data collection efforts and Jerry Guynes for preparing the TTUKa radars for deployment.

References

Acevedo, O. C., and Fitzjarrald, D. R.: The early evening surface-layer transition: temporal and spatial variability, J. Atmos. Soc., 58, 2650-2667, 2001.

Adaramola, M. S., and Krogstad, P.-Å.: Experimental investigation of wake effects on wind turbine performance, Renew. Energ., 36, 2078-2086, 2011.

Ahmad, T., Basit, A., Ahsan, M., Coupiac, O., Girard, N., Kazemtabrizi, B., and Matthews, P. C.: Implementation and analysis of yaw based coordinated control of wind farms, Energies, 12, 1266, 2019.

Allik, A., Uiga, J., and Annuk, A.: Deviations between wind speed data measured with nacelle-mounted anemometers on small wind turbines and anemometers mounted on measuring masts, Agron. Res., 12, 433-444, 2014.

Annoni, J., Gebraad, P. M., Scholbrock, A. K., Fleming, P. A., van Wingerden, J. W.: Analysis of axial-induction-based wind plant control using an engineering and a high-order wind plant model, Wind Energ., 19, 1135-1150, 2015.

Barnes, S. L.: A technique for maximizing details in numerical weather analysis, J. Appl. Meteor., 3, 396-409, 1964.

Barthelmie, R. J., Frandsen, S. T., Nielsen, M. N., Pryor, S. C., Rethore, P.-E., and Jørgensen, H. E.: Modelling and measurements of power losses and turbulence intensity in wind turbine wakes at Middelgrunden offshore wind farm, Wind Energ., 10, 517-528, 2007.

Barthelmie, R. J., and Jensen, L. E.: Evaluation of wind farm efficiency and wind turbine wakes at the Nysted offshore wind farm, Wind Energ., 13, 573-586, 2010.

Barthelmie, R. J., Pryor, S. C., Frandsen, S. T., Hansen, K. S., Schepers, J. G., Rados, K., Schlez, W., Neubert, A., Jensen, L. E., and Neckelmann, S.: Quantifying the impact of wind turbine wakes on power output at offshore wind farms, J. Atmos. Oceanic. Technol., 27, 1302-1317, 2010.

Barthelmie, R. J., Hansen, K. S., and Pryor, S. C.: Meteorological controls on wind turbine wakes, in Proceedings of the IEEE, 101, 1010-1019, 2013.

Bartl, J., Mühle, F., and Sætran, L.: Wind tunnel study on power output and yaw moments for two yaw-controlled model turbines, Wind Energ. Sci., 3, 489-502, 2018.

Bastankhah, M., and Porté-Agel, F.: Wind farm power optimization via yaw angle control: a wind tunnel study, J. Renew. Sustain. Energ., 11, 023301, 2019.

Burton, T., Sharpe, D., Jenkins, N., and Bossanyi, E.: Wind energy handbook, John Wiley & Sons Ltd., West-Sussex, United Kingdom, 642 pp, 2001.

Corten, G., and Schaak, P.: Heat and flux: increase of wind farm production by reduction of the axial induction, in Proceedings of the European Wind Energy Conference, Madrid, Spain, 2003.

Dahlberg, J. Å., and Thor, S.-E.: Power performance and wake effects in the closely spaced Lillgrund offshore wind farm, in: Extended Abstracts, European Offshore Wind Conference, Stockholm, Sweden, 2009.

Davies-Jones, R. P.: Dual-Doppler radar coverage as a function of measurement accuracy and spatial resolution, J. Appl. Meteor., 18, 1229-1233, 1979.

De-Prada-Gil, M., Alías, C. G., Gomis-Bellmunt, O., and Sumper, A.: Maximum wind power plant generation by reducing the wake effect, Energ. Convers. Manage., 101, 73-84, 2015.

Deardorff, J.W.: Numerical investigation of neutral and unstable planetary boundary layers, J. Atmos. Sci., 29, 91-115, 1972.

Drobinski, P., and Foster, R. C.: On the origin of near-surface streaks in the neutrally-stratified planetary boundary layer, Bound.-Layer Meteor., 108, 247-256, 2003.

Duncan, J. B., Hirth, B. D., and Schroeder, J. L.: Enhanced estimation of boundary layer advective properties to improve space-to-time conversion processes for wind energy applications, Wind Energ., 22, 1203-1218, 2019.

Edwards, J. M., Beare, R. J., and Lapworth, A.J.: Simulation of the observed evening transition and nocturnal boundary layers: single-column modelling, Quart. J. Roy. Meteor. Soc., 132, 61-80, 2006.

El-Asha, S., Zhan, L., and Iungo, G. V.: Quantification of power losses due to wind turbine wake interaction through SCADA, meteorological and wind LiDAR data, Wind Energ., 20, 1823-1839, 2017.

Fleming, P., Gebraad, P. M. O., Lee, S., van Wingerden, J. W., Johnson, K., Churchfield, M., Michalakes, J., Spalart, P., and Moriarty, P.: Simulation comparison of wake mitigation control strategies for a two-turbine case, Wind Energ., 18, 2135-2143, 2015.

Fleming, P., Annoni, J., Shah, J. J., Wang, L., Ananthan, S., Zhang, Z., Hutchings, K., Wang, P., Chen, W., and Chen, L.: Field test of wake steering at an offshore wind farm, Wind Energ. Sci., 2, 229-239, 2017a.

Fleming, P., Annoni, J., Scholbrock, A., Quon, E., Dana, S., Schreck, S., Raach, S., Haizmann, F., and Schlipf, D.: Full-scale field test of wake steering, in: J. Phys: Conf. Ser., 854, 012013, 2017b.

Fleming, P., Annoni, J., Churchfield, M., Martinez-Tossas L. A., Gruchalla, K., Lawson, M., and Moriarty, P.: A simulation study demonstrating the importance of large-scale trailing vortices in wake steering, Wind Energ. Sci., 3, 243-255, 2018.

Fleming, P., King, J., Dykes, K., Simley, E., Roadman, J., Scholbrock, A., Murphy, P., Lundquist, J. K., Moriarty, K., Fleming, K., van Dam, J., Bay, C., Mudafort, R., Lopez, H., Skopek, J., Scott, M., Ryan, B., Guernsey, C., and Brake, D.: Initial results from a field campaign of wake steering applied at a commercial wind farm: part 1, Wind Energ. Sci., 4, 273-285, 2019.

Foster, R. C.: Why rolls are prevalent in the hurricane boundary layer, J. Atmos. Sci., 63, 2647-2661, 2005.

Gebraad, P. M. O., and van Wingerden, J. W.: Maximum power-point tracking control for wind farms, Wind Energ., 18, 429-447, 2015.

Gebraad, P. M. O., Teeuwisse, F. W., van Wingerden, J. W., Fleming, P. A., Ruben, S. D., Marden, J. R., and Pao, L. Y.: Wind plant power optimization through yaw control using a parametric model for wake effects—a CFD simulation study, Wind Energ., 19, 95-114, 2016.

Gill, P. E., Murray, W., and Wright, M. H.: Practical Optimization, Academic Press, London, United Kingdom, 401 pp, 1981.

González-Longatt, F., Wall, P., and Terzija, V.: Wake effect in wind farm performance: steady-state and dynamic behaviour, Renew. Energ., 39, 329-338, 2012.

Hirth, B. D., Schroeder, J. L, Gunter, W. S., and Guynes, J. G.: Measuring a utility-scale wind turbine wake using the TTUKa mobile research radars, J. Atmos. Oceanic. Technol., 29, 765-771, 2012.

Deleted: in review

Hirth, B. D., and Schroeder, J. L.: Documenting wind speed and power deficits behind a utility-scale wind turbine, J. Appl. Meteor. Climatol., 52, 39-46, 2013.

Hirth, B. D., Schroeder, J. L., Gunter, W. S., and Guynes, J. G.: Coupling Doppler radar-derived wind maps with operational turbine data to document wind farm complex flows, Wind Energ., 18, 529-540, 2015.

Hirth, B. D., Schroeder, J. L., Irons, Z., and Walter, K.: Dual-Doppler measurements of a wind ramp event at an Oklahoma wind plant, Wind Energ., 19, 953-962, 2016.

Howland, M. F., Bossuyt, J., Martínez-Tossas, L. A., Meyers, J., and Meneveau, C.: Wake structure in actuator disk models of wind turbines in yaw under uniform inflow conditions, Renew. Energ. Sustain. Dev., 8, 043301, 2016.

Howland, M. F., Sanjiva, K. L., and Dabiri, J. O.: Wind farm power optimization through wake steering, in Proceedings of the Natl. Acad. Sci., 116, 14495-14500, 2019.

Jiménez, Á., Crespo, A., and Migoya, E.: Application of a LES technique to characterize the wake deflection of a wind turbine in yaw, Wind Energ., 13, 559-572, 2010.

Johnson, K. E., and Fritsch, G.: Assessment of extremum seeking control for wind farm energy production, Wind Eng., 36, 701-715, 2012.

Kanev, S. K., Savenije, F. J., and Engels, W. P.: An approach to optimize the lifetime operation of wind farms, Wind Energ., 21, 488-501, 2018.

Kim, S.-H., Shin, H.-K., Joo, Y.-C., and Kim, K.-H.: A study of the wake effects on the wind characteristics and fatigue loads for turbines in a wind farm, Renew. Energ., 74, 536-543, 2015.

Knudsen, T., Bak, T., and Svenstrup, M.: Survey of wind farm control—power and fatigue optimization, Wind Energ., 18, 1333-1351, 2015.

Lee, J., Son, E., Hwang, B., and Lee, S.: Blade pitch angle control for aerodynamic performance optimization of a wind farm, Renew. Energ., 54, 124-130, 2013.

Lee, J. C., and Lundquist, J. K.: Observing and simulating wind-turbine wakes during the evening transition, Bound.-Layer Meteor., 164, 449-474, 2017.

Lhermitte, R. M.: Measurement of wind and wind field by microwave Doppler radar techniques, Atmos. Environ., 5, 691-694, 1971.

Lin, C. L., McWilliams, J. C., Moeng, C. H., and Sullivan, P. P.: Coherent structures and dynamics in a neutrally stratified planetary boundary layer flow, Phys. Fluids, 8, 2626-2639, 1996.

Lorsolo, S., Schroeder, J. L., Dodge, P., and Marks, F.: An observational study of hurricane boundary layer small-scale coherent structures, Mon. Weath. Rev., 136, 2871-2893, 2008.

Machefaux, E., Larsen, G. C., Koblitz, T., Troldborg, N., Kelly, M. C., Chougule, A., Hansen, K. S., and Rodrigo, J. S.: An experimental and numerical study of the atmospheric stability impact on wind turbine wakes, Wind Energ., 19, 1785-1805, 2016.

Mahrt, L.: The early evening boundary layer transition, Quart. J. Roy. Meteor. Soc., 107, 329-343, 1981.

Manwell, J. F., McGowan, J. G., and Rogers, A. L.: Wind energy explained: theory, design, and application, Second Edition, John Wiley & Sons Ltd., West-Sussex, United Kingdom, 689 pp, 2009.

Marathe, N., Swift, A., Hirth, B., Walker, R., and Schroeder, J.: Characterizing power performance and wake of a wind turbine under yaw and blade pitch, Wind Energ., 19, 963-978, 2016.

McKay, P., Carriveau, R., and Ting, D. S-K.: Wake impacts on downstream wind turbine performance and yaw misalignment, Wind Energ., 16, 221-234, 2012.

Mittelmeier, N., and Kühn, M.: Determination of optimal wind turbine alignment into the wind and detection of alignment changes with SCADA data, Wind Energ. Sci., 3, 395-408, 2018.

Morrison, I., Businger, S., Marks, F., Dodge, P., and Businger, J. A.: An observational case for the prevalence of roll vortices in the hurricane boundary layer, J. Atmos. Sci., 62, 2662-2673, 2005.

Nieuwstadt, F. T. M., and Brost, R. A.: The decay of convective turbulence, J. Atmos. Sci., 43, 532-546, 1986.

Park, J., and Law, K. H.: Cooperative wind turbine control for maximizing wind farm power using sequential convex programming, Energ. Conv. Manage., 101, 295-316, 2015.

Park, J., and Law, K. H.: A data-driven, cooperative wind farm control to maximize the total power production, Appl. Energ., 165, 151-165, 2016.

Parkin, P., Holm, R., and Medici, D.: The application of PIV to the wake of a wind turbine in yaw, in: Proceedings of the 4th International Symposium on Particle Image Velocimetry, Göttingen, 2001.

Schepers, J. G., Obdam, T. S., and Prospathopoulos, J.: Analysis of wake measurements from the ECN wind turbine test site Wieringermeer, EWTW, Wind Energ., 15, 575-591, 2012.

Schottler, J., Mühle, F., Bartl, J., Peinke, J., Adaramola, M. S., Sætran, L., and Hölling, M.: Comparative study on the wake deflection behind yawed wind turbine models, in J. Phys.: Conf. Ser., 854, 012032, 2017.

Sørensen, T., Nielsen, P., and Thøgersen, M. T.: Recalibrating wind turbine wake model parameters—validating the wake model performance for large offshore wind farms, in: Proceedings of the European Wind Energy Conference and Exhibition, Athens, Greece, 2006.

Subramanian, B., Chokani, N., and Abhari, R. S.: Impact of atmospheric stability on wind turbine wake evolution, J. Wind Eng. Ind. Aerod., 176, 174-182, 2018.

Träumner, K., Damian, T., Stawiarski, C., and Wieser, A.: Turbulent structures and coherence in the atmospheric surface layer, Bound.-Layer Meteor., 154, 1-25, 2015.

Trujillo, J. J., Seifert, J. K., Würth, I., Schlipf, D. and Kühn, M.: Full-field assessment of wind turbine near-wake deviation in relation to yaw misalignment, Wind Energ. Sci., 1, 41-53, 2016.

Van der Hoek, D., Kanev, S., Allin, J., Bieniek, D., and Mittelmeier, N.: Effects of axial induction control on wind farm energy production—a field test, Renew. Energ., 140, 994-1003, 2019.

Vollmer, L., Steinfeld, G., Heinemann, D., and Kühn, M.: Estimating the wake deflection downstream of a wind turbine in different atmospheric stabilities: an LES study, Wind Energ. Sci., 1, 129-141, 2016.

Formatted: Justified, Line spacing: 1.5 lines

Deleted: ¶

Page 3: [1] Deleted	**Duncan, James B**	**1/27/20 8:13:00 PM**
Page 4: [2] Deleted	**Duncan, James B**	**1/27/20 8:13:00 PM**
Page 9: [3] Deleted	**Duncan, James B**	**1/27/20 8:13:00 PM**
Page 27: [4] Deleted	**Duncan, James B**	**1/27/20 8:13:00 PM**